

Series 08    Astrodynamics and  
Satellite Systems 02

# **GPS-Antenna Phase Center Measurements Performed in an Anechoic Chamber**

*G.A. Bartels*



Delft University Press



706713

# GPS-Antenna Phase Center Measurements Performed in an Anechoic Chamber

Bibliotheek TU Delft



C 3021892

2392  
334  
0

**Series 08: Astrodynamics and  
Satellite Systems**

**02**

# GPS-Antenna Phase Center Measurements Performed in an Anechoic Chamber

*G.A. Bartels*



Delft University Press / 1997

*Published and distributed by:*

Delft University Press  
Mekelweg 4  
2628 CD Delft  
The Netherlands  
Telephone +31 (0)15 278 32 54  
Fax +31 (0)15 278 16 61  
e-mail: DUP@DUP.TUdelft.NL

*by order of:*

Faculty of Aerospace Engineering  
Delft University of Technology  
Kluyverweg 1  
P.O. Box 5058  
2600 GB Delft  
The Netherlands  
Telephone +31 (0)15 278 14 55  
Fax +31 (0)15 278 18 22  
e-mail: Secretariaat@LR.TUdelft.NL  
website: <http://www.lr.tudelft.nl>

*Cover:* Aerospace Design Studio, 66.5 x 45.5 cm, by:  
Fer Hakkaart, Dullenbakkersteeg 3, 2312 HP Leiden, The Netherlands  
Tel. +31 (0)71 512 67 25

90-407-1596-3

Copyright © 1997 by Faculty of Aerospace Engineering

All rights reserved.

No part of the material protected by this copyright notice may be reproduced or utilized in any form or by any means, electronic or mechanical, including photocopying, recording or by any information storage and retrieval system, without written permission from the publisher: Delft University Press.

Printed in The Netherlands

# Contents

1.	Introduction	1
2.	Antennas	5
2.1	Introduction	5
2.2	Antenna phase center	8
2.3	Phase center determination	11
2.4	GPS antennas used for tests	13
3.	Phase center measurements	17
3.1	The anechoic chamber DUCAT	17
3.2	Results of phase center measurement	21
3.3	Comparison with former phase center measurements	33
4.	Baseline results with different antennas	39
4.1	Introduction	39
4.2	Mixed-baseline results	41
4.3	Mixed-baseline results of former studies	45
4.4	Discussion	53
5.	Conclusions and Recommendations	59
5.1	Conclusions	59
5.2	Recommendations	60
6.	References	63



# Preface

Over the last decade GPS has become an important tool for high-precision geodesy, in particular for research in geophysics and geodynamics. For this purpose, several manufacturers have developed special receivers and antennas which are designed to provide millimeter-accuracy range measurements on the carrier signals. Experience has shown that these measurements can be exploited to achieve relative positioning accuracies at the few millimeter level for extended networks of GPS receivers. However, this was only possible when identical equipment was used at all points of the network. The main reason for this requirement is due to the differences in the various antenna designs. They are all good, but not perfect, approximations of the 'ideal' antenna. This would nominally have a spherical radiation pattern, originating from a fixed 'antenna phase center', while the phase center of the 'real' antenna exhibits small variations as a function of the direction of the signal relative to the antenna. When using 'identical' antennas, most of the imperfections cancel in the relative position determinations. When different antenna types (of different manufacturers) are mixed, this may lead to significant errors, however, in particular in the height component. For two antenna types, which are currently very commonly used (Rogue/TurboRogue and Trimble-4000), this error may become as large as 8 cm in height. Still, antenna mixing will be almost unavoidable, in particular in larger networks involving different participating groups and also when combining different networks. In that case, the only solution is to take the various antenna characteristics into account during the data analysis. Therefore, accurate models of the phase center variations of the various antenna types are required.

The need for such models was corroborated by the fact that the Faculty of Aerospace Engineering and the Faculty of Geodesy of Delft University of Technology (DUT) together operate a permanent (SNR-8 Rogue) receiver at the Kootwijk Observatory for Satellite Geodesy (KOSG). This is one of the global stations of the International GPS Service for geodynamics (IGS), and therefore the main reference point for geodetic measurements in the Netherlands. In this function, the station is frequently 'visited' by other receivers which are slaved to the Rogue reference point through local surveys and phase antenna center definitions. In 1993 several receivers were tested in Kootwijk simultaneously, providing valuable measurement data to verify phase center variation models. These can only be obtained by actually measuring the variations, for example at an antenna test range or in an anechoic chamber. Significant results have already been reported by several investigators, but it was felt that additional tests and an independent verification using different hardware and test facilities would be useful.

Therefore, at the initiative of the Faculty of Aerospace Engineering, a cooperative test project was organized at DUT, in which three Faculties participated; the measurements were performed in the anechoic chamber (DUCAT) of the Faculty of Electrical Engineering using test antennas (TurboRogue and Trimble-4000) provided by the Faculty of Geodesy. The data analysis was performed at the Faculty of Aerospace Engineering.

In this report, the results of the antenna measurements and the effect of their application in

the GPS data analyses are presented. In general the measurements confirm the results of other investigators and the differences between 'identical' antennas seem to be small. Apart from the expected phase center variations, it was found that the definition of the 'reference' phase center is dependent of the range of elevations that is considered in the analyses. It is shown that the accuracy of the positioning results improves significantly if the phase center variations are modeled.

This investigation was also motivated by the EC project for the study of Geodynamics of South-East Asia (GEODYSSSEA), in which our group has the prime responsibility for the analysis of the GPS measurements. This project comprises a network of about 40 sites in South-East Asia, which were observed with Trimble-4000 SSE receivers during the first campaign in November/December 1994. In addition there are some 5 to 10 permanent IGS stations in the area, equipped with Rogue and TurboRogue receivers. It is intended to provide an good connection between these networks, which is only feasible when the different antenna phase centers are accurately defined. The project described in this report has provided the necessary understanding of the problem and models for the phase center variations of the Trimble and TurboRogue antenna types which can be readily applied.

# Acknowledgements

This study has been performed under supervision of ir. B.A.C. Ambrosius, ir. T.A. Springer and ir. M. Hajian. I would like to thank them for their guidance and the pleasant cooperation. Also I wish to thank prof.dr.ir. L.P. Ligthart of the Department of Telecommunications and Remote Sensing Technology, the Faculty of Electrical Engineering, for offering me the possibility to perform antenna measurements in the anechoic chamber. Furthermore, I would like to thank ir. D.L.F. van Loon of the Kootwijk Observatory for Satellite Geodesy and ir. G.J. Husti of the Faculty of Geodesy for providing me the GPS antennas.



# 1. Introduction

The application of GPS for geodetic purposes demands a high-accuracy position determination. For this reason, GPS antennas have to be well calibrated. One of the most important questions that may be asked concerning antennas is: "In which point of the antenna is the signal received, and where is this point located with respect to the physical center of the antenna?" The point which the measurements refer to is defined as the phase center of the antenna. The antenna phase center is a point in the antenna which position depends of the elevation and azimuth observation angle. When antennas are involved in the measurements, one must know where the phase center is located.

The GPS satellites transmit two carrier signals with different frequencies. The two carrier signals, denoted L1 and L2, are:

$$L1 : f_1 = 1575.42 \text{ MHz}$$

$$L2 : f_2 = 1227.60 \text{ MHz}$$

The signals, on their path between satellites and ground stations, propagate through atmospheric regions of different nature and variable state, and experience different kinds of influences. Variations may occur in the direction of propagation, in the velocity of propagation and in the signal strength. For the user who is interested in the undisturbed signal the atmosphere appears as an unwanted perturbation. The impacts on the observations are, in many cases, much larger than the accuracy required in satellite geodesy. Consequently, the atmospheric influences have to be considered within the parameter estimation process. The GPS signals, when propagating from the satellite antenna to the user antenna are subject to the following propagation effects (Figure 1.1):

- propagation delay in the ionosphere
- propagation delay in the troposphere

With the presence of free electrons in the ionosphere and molecules in the troposphere, the propagation velocity of the signal differs from the velocity of light, resulting in a propagation delay of the signal. Consequently, the range between satellite and receiver will differ from the real range.

The propagation delay in the ionosphere depends on the electron content along the signal path and on the frequency used. This results in different observations for the L1 and L2 signals. The effect of the ionosphere can be eliminated by using dual frequency measurements. Combining observations on L1 and L2 in an intelligent way yields the ionospheric free linear combination, also referred to as L3.

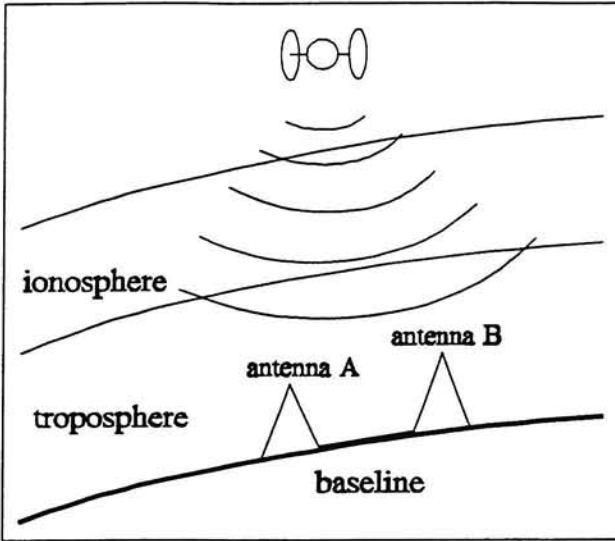


**Figure 1.1:** Propagation effects in the atmosphere.

The tropospheric delay is a function of the distance travelled by the electromagnetic signal through the neutral atmosphere. The distance to be travelled by the signal before reaching the observing station is a function of the elevation of the satellite. Therefore, the tropospheric delay for a satellite at elevation  $E$  is often written as the product of the delay at zenith ( $E=90^\circ$ ) and a mapping function which relates this zenith delay to the delay at elevation  $E$ :

$$\Delta r = F(E) \cdot \Delta r(90^\circ) \quad (1.1)$$

where:

$F(E)$  mapping function to relate the zenith delay to  $\Delta r(E)$ .  
 Note that  $F(90^\circ)$  should be equal to one.

The troposphere propagation delay is difficult to determinate, because the tropospheric influence can variate strongly over large distances. If two receivers are relatively close together, tropospheric influences are very similar for the received signals. The tropospheric error almost completely disappears by differencing the observations from the different

receivers. So normally there is no need to estimate the tropospheric parameters for short distances. When receiver distances are larger than about 50 km [4], the local tropospheric conditions are no longer sufficiently correlated with one another. In this case the troposphere for each receiver has to be described with a model using equation (1.1). In this model the tropospheric parameters are estimated. Considering a short baseline with different GPS antennas, large differences in the vertical component of the baseline estimates may occur if troposphere corrections are estimated. The reason for this effect are the elevation dependent phase center variations that do not cancel for baselines with different antennas. This variation being such that it is interpreted by the GPS processing software as a tropospheric delay if tropospheric delay parameters are estimated. The reason why the variation is interpreted as a tropospheric delay is because the antenna phase center and the tropospheric delay are both elevation dependent, and therefore strongly correlated. This effect was first noted by scientists from the University of Berne when Trimble antennas were mixed with Rogue and Ashtech antennas.

Up to now very little effort has been put in the modelling of the phase center problem of different types of GPS antennas. Schupler et al. [11] and ESTEC [13] performed some phase center measurements with GPS antennas. To avoid the vertical baseline error when mixed antennas are involved, a more well founded knowledge of the phase center of the different antennas is desired. Consequently, the main target in this study is the determination of the elevation and azimuth dependent phase center variations of different antennas obtained by measurements in an anechoic chamber. For this purpose a set of GPS data and two different GPS antennas were available. The data were collected in May 1993 with Rogue, TurboRogue, Trimble SSE and SST receivers located at Delft and Kootwijk. A TurboRogue and a Trimble 4000ST antenna were used for phase center measurements performed in the anechoic chamber of the Delft University of Technology, DUCAT.

This report will first give a description of antennas, especially antennas for GPS use. In chapter 3 the results of the phase center measurements performed at DUCAT are given and compared with other phase center measurements. Chapter 4 will provide the results of the mixed-baseline estimates at Delft and Kootwijk obtained from the data processing. Finally, the conclusions and recommendations will be presented in chapter 5.



# 2. Antennas

## 2.1 Introduction

An antenna usually is defined as "a means for radiating or receiving radio waves". In other words, the antenna is the transitional structure between free-space and a guiding device, as shown in Figure 2.1. The guiding device or transmission line may take the form of a coaxial line or a hollow pipe (waveguide), and is used to transport electromagnetic energy from the transmitting source to the antenna, or from the antenna to the receiver. In the former case we have a transmitting antenna and in the latter a receiving antenna. When discussing an antenna, one usually describes its properties as a transmitting antenna. From the reciprocity theorem [6] however, the characteristics of the antenna in a receiving situation are identical with the characteristics of the antenna in a transmitting situation.

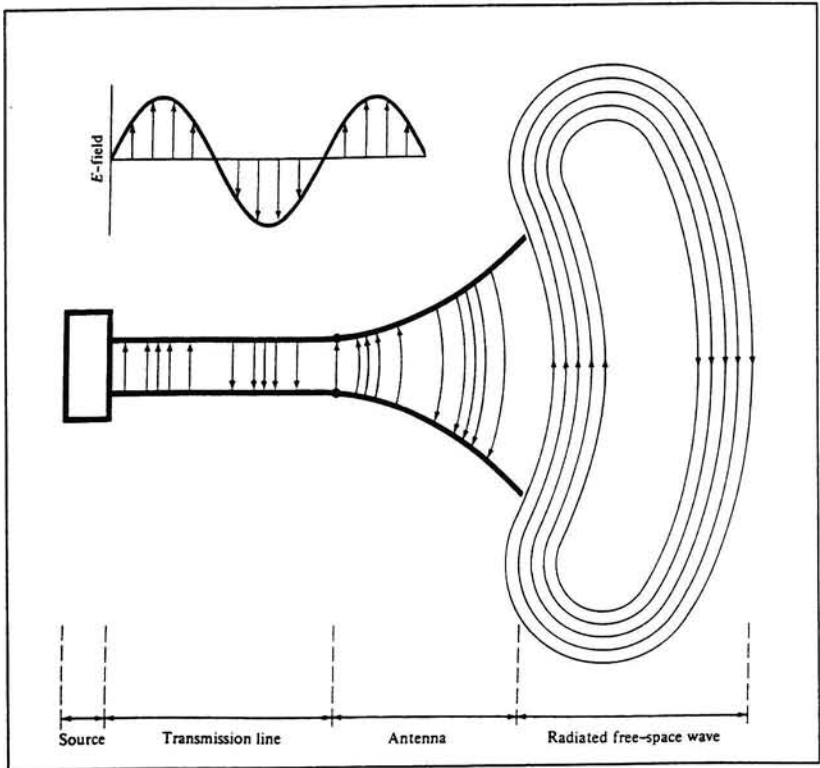
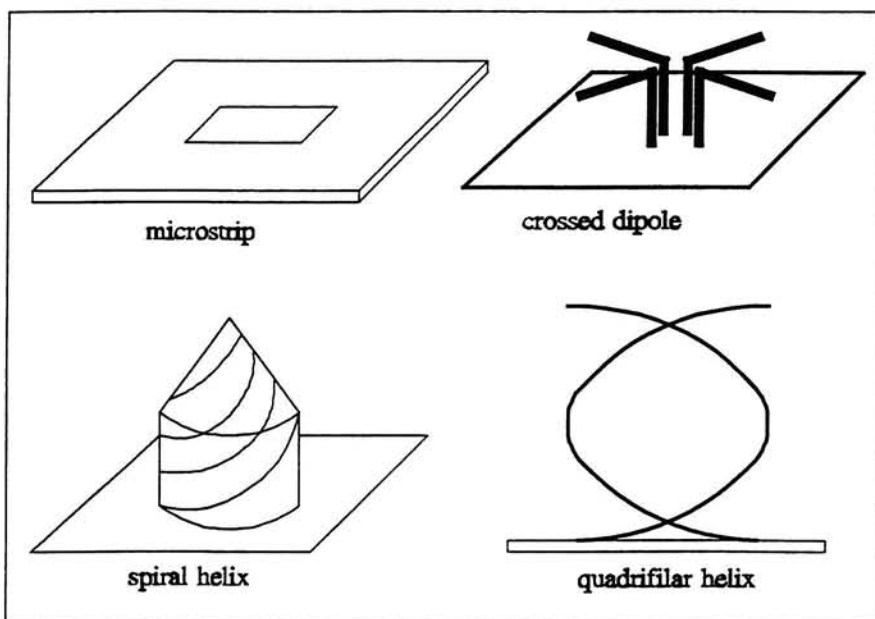


Figure 2.1: Antenna as a transition device.

Since antennas play a very important part in GPS, it is essential to have a thorough understanding of the principles on which they perform their task efficiently. In practice, this has led to the design and development of a great many different types of antennas each suited to a particular set of applications. Several different types of antennas are presently available in GPS systems (see Figure 2.2). These may be generally categorized as:

- monopole and crossed dipole configurations
- quadrifilar helices or volutes
- microstrip antenna
- tapered or spiral helices



**Figure 2.2:** Different antenna types used for GPS receivers.

The GPS-signals are required to be circularly polarized, because the ionosphere causes a rotation of the polarization of the signal. Circular polarization avoids this phenomenon. Circular polarization can be achieved when the magnitudes of the two components  $E_x$  and  $E_y$  of the electric field  $E$  of the electromagnetic wave are the same and the time-phase difference between them is an odd multiple of  $\pi/2$ , see Figure 2.3.

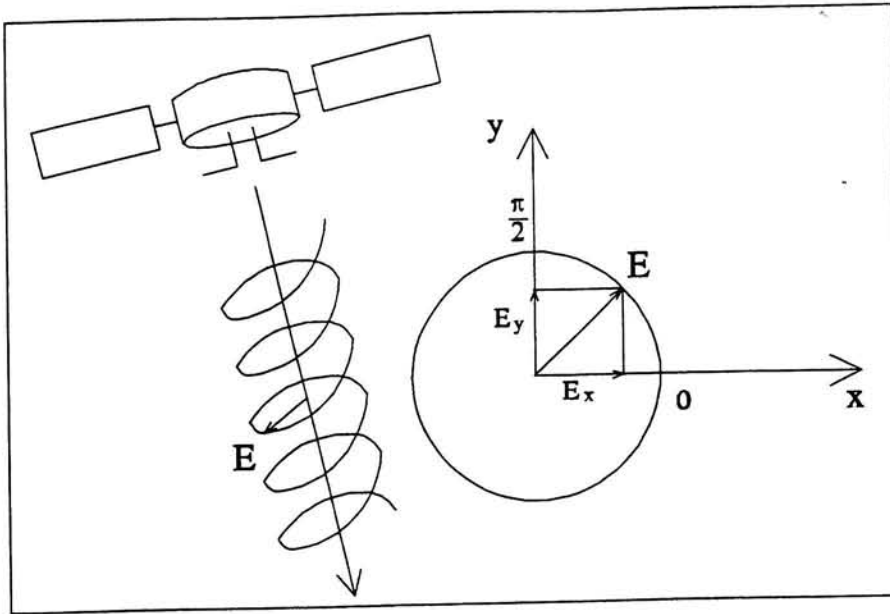


**Figure 2.3:** Circular polarization.

The direction properties of an antenna are represented in a radiation intensity pattern. With the radiation intensity pattern the power can be determined from an incoming signal as a function of the elevation and azimuth. Figure 2.4 gives an example of a radiation pattern of a dipole antenna. In the radiation pattern the directive gain  $D$  (that is the ratio of the radiation intensity in that direction to the total radiated power) is given as a function of the elevation and azimuth of the incoming signal.  $D_{\max}$  is the value of the directive gain in the direction of its maximum value. In cases where the antenna radiation pattern is azimuth dependent, all antennas have to be orientated prior to the survey. For this reason, antennas have an orientation mark directed to magnetic north. If an antenna has to be suitable for reception of GPS-signals, some demands have to be made on the radiation pattern. The GPS antenna has to be very sensitive because of the rather weak signal and must allow signal reception from all elevations and azimuths of the visible hemisphere. The radiation pattern has to be in those directions as powerful as possible. To avoid reception of reflected satellite signals from the ground, the radiation pattern in the direction of the ground has to be practically zero. To achieve these characteristics, a groundplane can be placed under the antenna. The shape of the pattern can be influenced by changing the height of the dipole above the groundplane and by changing the dimensions of the groundplane.

The complete radiation pattern demonstrates at given polarization and frequency the relative amplitude and the phase of the field at infinite distance (far-field region) of the antenna. For geodetic applications the phase pattern of the antenna is of importance. If the wavefront is circular, one point can be indicated as the phase center of the antenna. If the wavefront is not circular, there is a problem, because in that case it is not possible to indicate one point as the phase center.

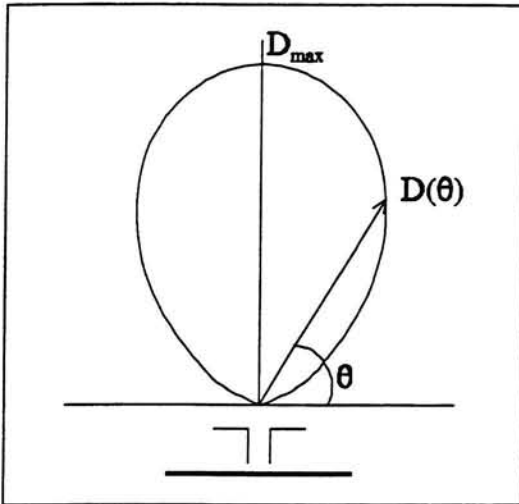


Figure 2.4: Radiation pattern.

## 2.2 Antenna phase center

An important aspect of an antenna is the position of the phase center. The most exact definition for the phase center of an antenna is that it is the apparent source of radiation and is generally not identical with the physical antenna center. It is desirable to assign to the antenna a reference point such that for a given frequency, the variation of the phase is independent of elevation and azimuth. This reference point is known as the phase center of the antenna. It is evident that only an ideal point source radiator will exhibit a fixed phase center since it produces a truly spherical phasefront, see Figure 2.5.

In practice, no antenna is a point source with ideal spherical wavefronts. Any finite-size radiating source will generate equiphasic contours which are not entirely spherical but rather 'dimpled' or distorted. In that case we may examine small near-spherical portions of the wavefront with a corresponding center for each spherical portion. A single phase center valid for all values of elevation ( $\theta$ ) and azimuth ( $\phi$ ) does not exist. The phase

center is thus not constant but is dependent upon the observation angle, see Figure 2.6. Therefore, the theoretical definition of the phase center must be transformed into a practical definition.

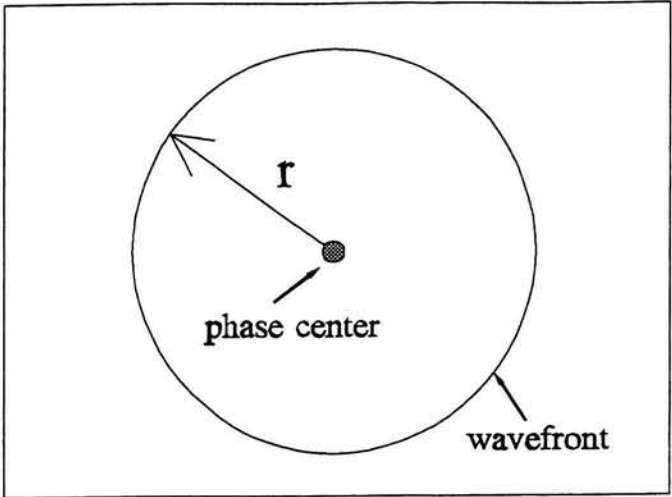


Figure 2.5: Ideal point source radiator.

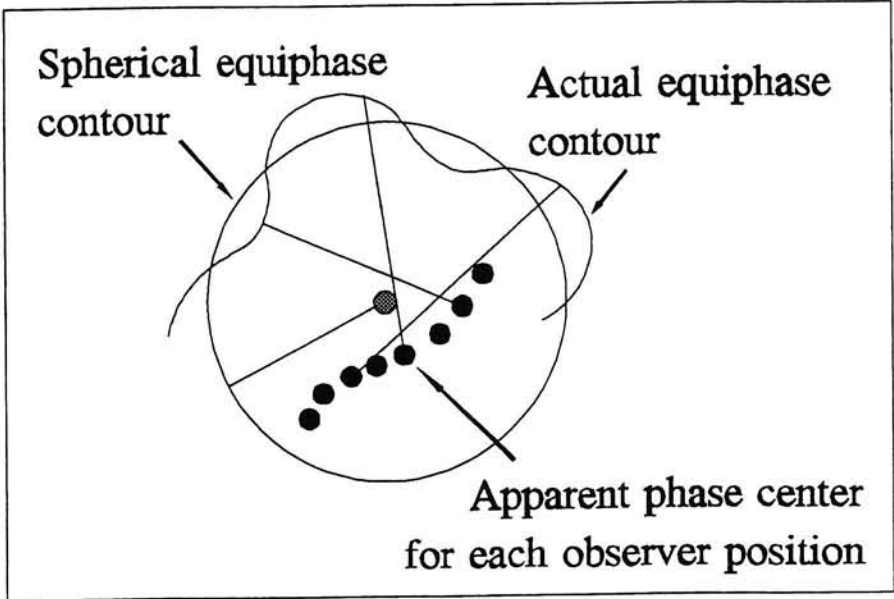


Figure 2.6: Angle dependent phase center.

Based on the theoretical definition of the phase center an antenna reference point can be chosen with at certain distance (far-field region) an imaginary sphere. At the sphere the phase difference, that is, the difference between the measured phase and the calculated phase, can be determined. If the antenna were an ideal point source radiator, the measured phase difference would be constant at every point located on the sphere. Considering a finite-size antenna, the measured phase difference is not constant. A geometrical figure is imaginable in which the phase difference is constant. This figure is an approximation of the sphere, see Figure 2.7. By measuring the phase difference at different elevation  $\theta$  and azimuth  $\phi$ , a phase difference function  $\Delta\Phi(\theta,\phi)$  can be described. This function can be converted in an antenna delay function, in which the measured phase difference is transformed in a distance difference:

$$\Delta d(\theta,\phi) = \frac{c}{f} \Delta\Phi(\theta,\phi) \tag{2.1}$$

with:

- c velocity of light
- f frequency

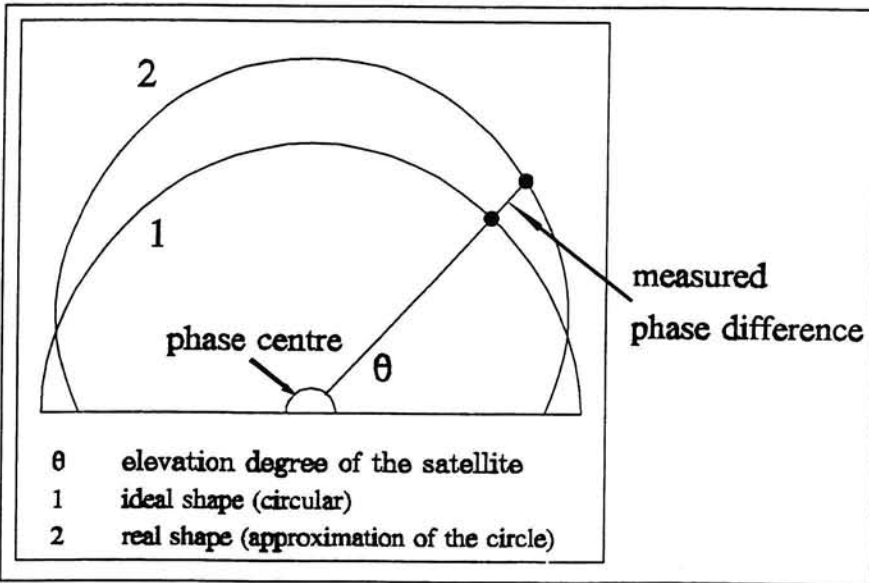


Figure 2.7: Approximation of equiphase sphere.

When the antenna delay function is known, the observations can be corrected for the antenna influences. The antenna delay function can be determined in an anechoic chamber, which is discussed in the next section.

## 2.3 Phase center determination

Since the antenna is not an ideal point source, a search has to be made to find the position which shows the minimum phase shift variation; the phase center. An approximate experimental technique for determination of the phase center location with its corresponding antenna delay function (see 2.2) involves recording the phase pattern as the antenna is rotated about an axis, simulating elevation, see Figure 2.8. A search is made to find a point for which the phase variations of the phase pattern are minimized in some sense. The movement of the phase center, that is, the phase center variation, will be related to the relative smoothness or distortion of the phasefront; the smoother (near spherical) the phasefront the smaller the phase center movement. This technique produces a 'weighted average' phase center position. Considering the phase center determination, two things must be distinguished: the constant (averaged) phase center offset and the phase center variation. The following sequence describes how the phase center of an antenna is determined.

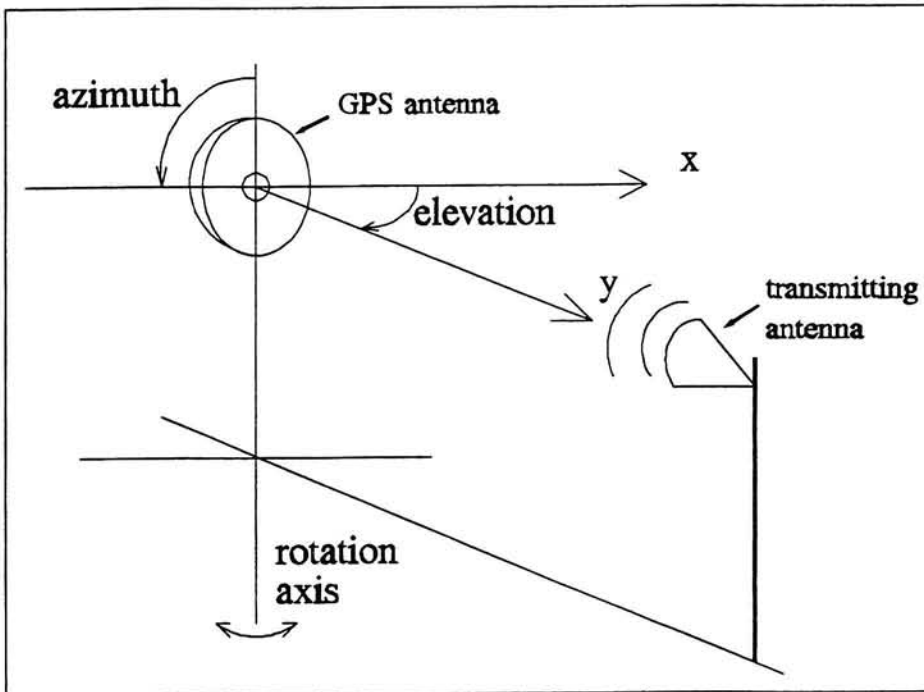
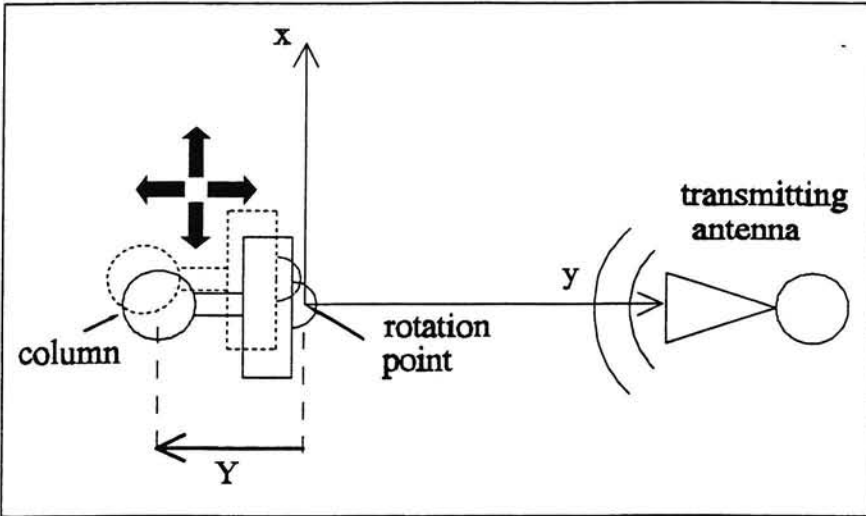


Figure 2.8: Rotation of the antenna simulating elevation and azimuth.

The first step in the antenna measurement procedure is to determine the phase variation of a chosen point at the rotation-axis of the antenna. Series of phase pattern measurements are recorded while the antenna is rotated  $\pm 90^\circ$  about the elevation axis. The phase pattern of a different chosen point is compared with the previous one. This point is also at the rotation-axis, but with respect to the antenna its position is at a different spot. The antenna is moved along the x and y axis until the position with the minimum phase change variation is found (Figure 2.9).



**Figure 2.9:** Searching the phase center by moving the antenna.

This places the phase center of the antenna at the axis of rotation. The x value is found at the situation where the curve for the best symmetrical phase pattern is produced, and the y value is found at the situation where the minimum phase shift variation is produced. By reading the x and y value, the offsets of the phase center of the antenna with respect to the column-axis are determined. The distance between the column-axis and the front-plane of the antenna is subtracted from the determined y value, resulting in the vertical offset of the phase center with respect to the front plane of the antenna, see Figure 2.9.

The minimum phase center variation can only be found when the elevation-range of interest is taken into account. This is essential, because for a different elevation-range of interest a different minimum phase center variation pattern is found. In this study the minimum phase center variation is determined for the elevation-range of interest  $-75/75$  degrees. The reason why an elevation-range of interest of  $-75/75$  degrees is chosen, is because in GPS we are normally interested in phase observations above an 15 degrees elevation cut-off. Once the constant offsets of the phase center and its minimum phase shift variation are determined, the antenna is uncoupled from the positioner and moved in the azimuth ( $\phi$ ) direction and again rotated  $\pm 90^\circ$  about the elevation ( $\theta$ ) axis while recording the phase change, see Figure 2.8.

## 2.4 GPS-antennas used for tests

The GPS-antennas which are used for this study to collect the data are:

- the Rogue Dorne-Margolin B antenna
- the TurboRogue Dorne-Margolin T antenna
- the Trimble 4000ST antenna

The Rogue and TurboRogue antennas are dual-band crossed dipole antenna types mounted to a choke ring backplane. The omni-directional antennas track the L1 and L2 signals from all visible satellites. The crossed dipole antenna is simple in structure and may be considered as a short linear conductor, see Figure 2.10. The length  $L$  is short compared to wavelength  $\lambda$ . The short length results in a uniform current  $I$  along the entire length  $L$  of the dipole. The diameter  $d$  of the dipole is small compared to its length ( $d \ll L$ ).

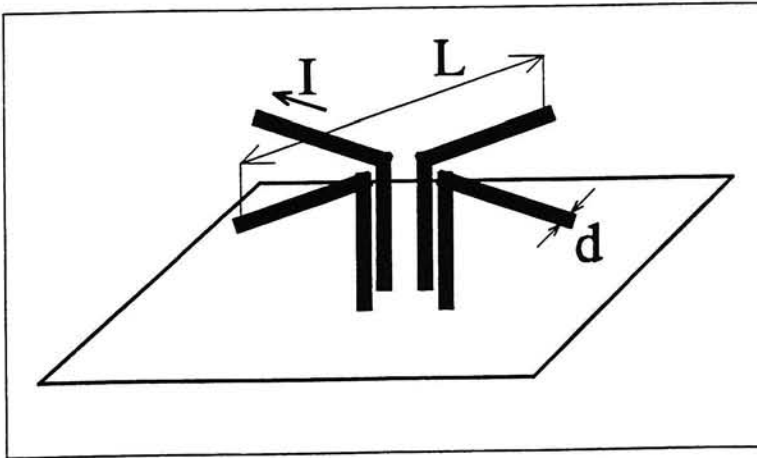


**Figure 2.10:** The crossed dipole.

The choke ring acts as an absorber to L-band radiation, serving to electrically isolate the antenna from nearby objects, and to suppress gain at low elevations where multipath signals are present, see Figure 2.11. These signals pass through an L-band preselection filter and a low noise amplifier prior to being sent via a coaxial cable to the down-converter assembly.

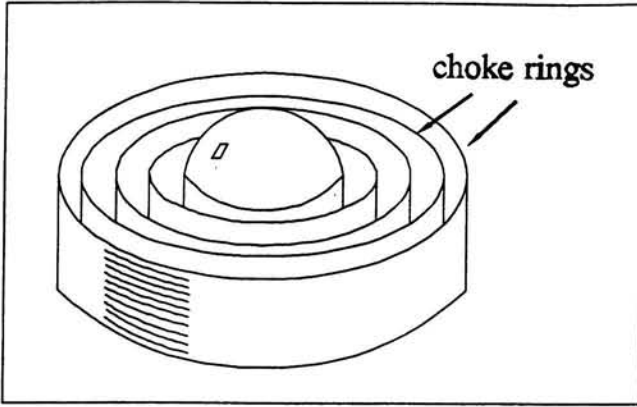


**Figure 2.11:** The choke ring.

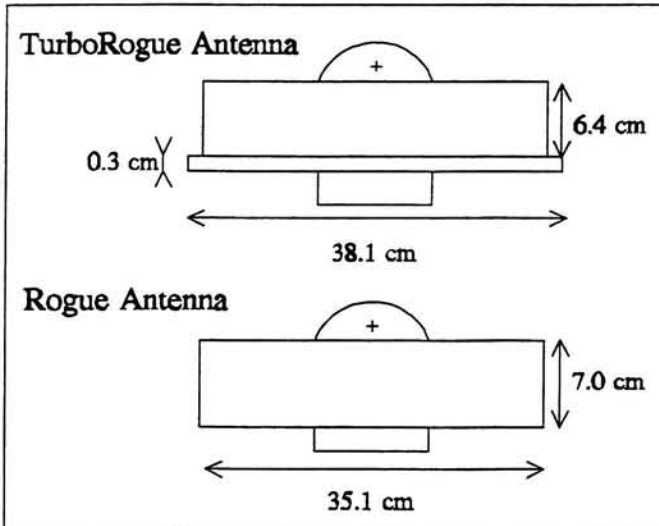


**Figure 2.12:** The TurboRogue and Rogue antenna.

The TurboRogue differs from the Rogue in the geometrical shape of the choke ring. Although the TurboRogue antenna is of the same type as the Rogue antenna, it does not mean that the antenna properties, in particular the phase center, are the same. Figure 2.12 illustrates the Rogue and TurboRogue antenna with their dimensions.

The Trimble 4000ST antenna belongs to the group of the microstrip antennas. Microstrip antennas are the most robust and simple in construction. They may be either single or dual frequency antennas with a very low profile which makes them ideal for airborne applications. Figure 2.13 gives an example of the microstrip antenna. Microstrip antennas consist of a very thin ( $t \ll \lambda$ ) metallic strip (patch) placed a small fraction of a wavelength ( $h \ll \lambda$ ) above the ground plane. The strip and the ground plane are separated by a dielectric sheet (referred to as the substrate). The radiating elements and the feed lines are usually photoetched on the dielectric substrate. The feed line is also a conducting strip, usually of smaller width. Because the thickness of the microstrip is usually very small, the waves generated within the dielectric substrate (between the patch and the ground plane) undergo considerable reflections when they arrive at the edge of the strip. Therefore only a small fraction of the available energy is radiated; thus the antenna is considered to be very inefficient, although this can be largely overcome by low noise preamplifiers.

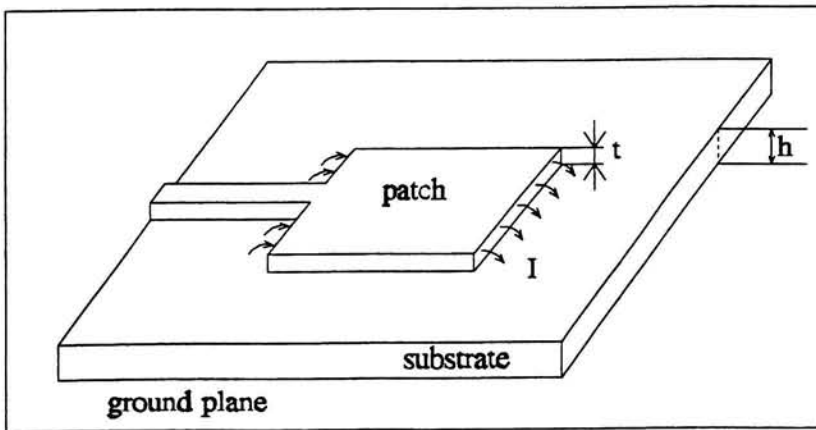


Figure 2.13: The microstrip antenna.

The ground plane isolates the antenna from nearby objects, and suppresses gain at low elevations where multipath signals are present. Figure 2.14 illustrates the Trimble 4000ST with its dimensions.

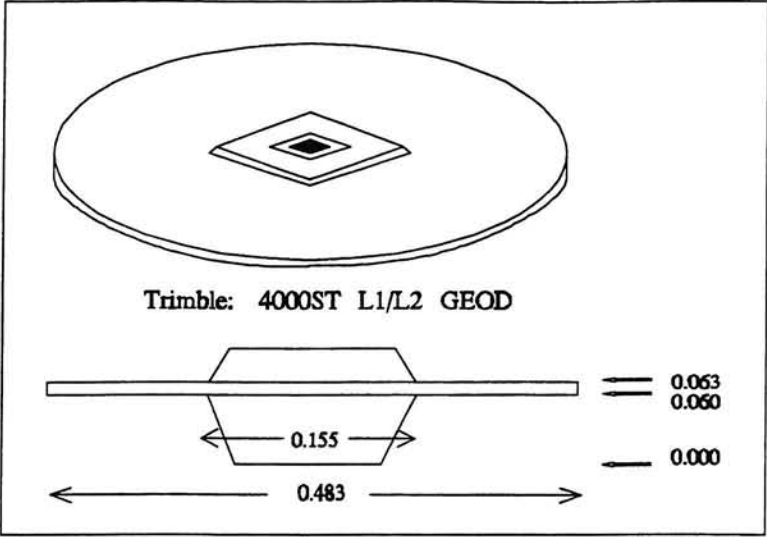


Figure 2.14: The Trimble 4000ST antenna.

### 3. Phase center measurements

#### 3.1 The anechoic chamber DUCAT

Within the Laboratory of Telecommunications and Remote Sensing Technology of the Department of Electrical Engineering, Delft University of Technology, there is an anechoic chamber of moderate size (3m \* 3m \* 6m, see Figure 3.1) which is called DUCAT; Delft University Chamber for Antenna Tests. The chamber is a large unobstructed volume which is free of any unwanted reflecting objects and electromagnetically interfering signals. The anechoic chamber developed as a practically realizable environment, achieves, within limits, many of the wanted requirements. The 'free space' condition (free space implies remoteness from any material substances from which waves may be reflected) is reached by creating an area in which unwanted reflections from the walls are small in amplitude compared to the direct test signal. The low reflectance can be achieved by use of electromagnetic wave absorbers which cover all of the reflecting surfaces (walls, ceiling, floor and positioning bodies) within the chamber. Before the absorbers were placed the entire chamber was covered with copper plate thus forming a cage of Faraday. To maintain a completely shielded chamber the doors are of a special design. They are not supported upon hinges but they are pulled in straight by pneumatic cylinders. The shielding of the chamber is for frequencies above 2 GHz up to 18 GHz. Notice that the frequencies used for the measurements presented here are below the 2 GHz. This home-made design was build in 1979, and was initially used for far-field measurements of antennas small relative to their wavelength. Since 1989 the laboratory is also preparing research on near-field antenna measurements in this anechoic chamber. The characteristics of DUCAT are given in Table 3.1.

**Table 3.1:** Characteristics of DUCAT

* Shielding (2 - 18 GHz)	120 dB
* Absorbers 3 m walls	AFP 18
by Plessey other side walls	AFP 6
* Reflection one side	-36 dB
* Positioner distance	3.5 m
* Axes resolution positioners	
azimuth axis (here: elevation)	0.006°/step
x-axis	10µm/step
y-axis	10µm/step
* Instrumentation	
Noise floor	-125 dBm
Dynamic range netw. analyzer	100 dB
Inter channel isolation	60 dB
S/N ratio reference signal	65 dB

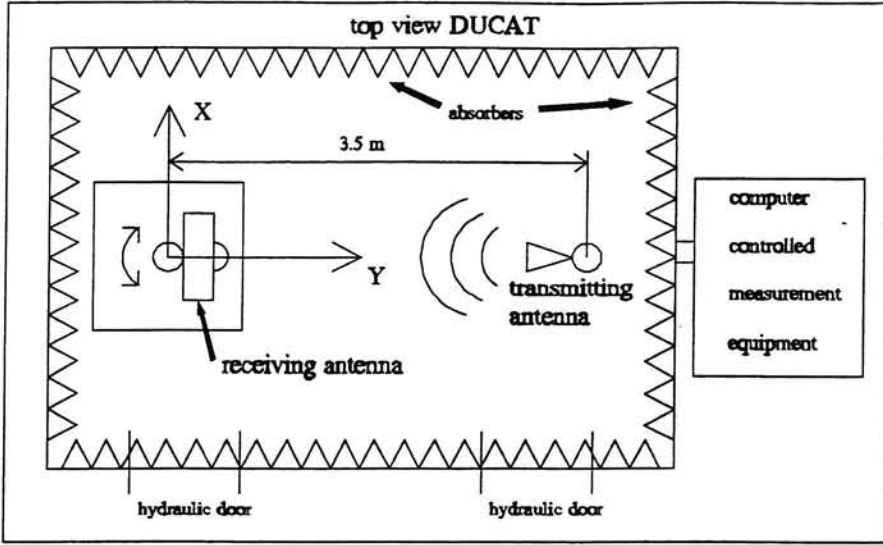


Figure 3.1: Top view of the anechoic chamber.

In this study we are interested in the phase of the signal in the far-field region, because in the far-field region antenna measurements are independent of the distance between the transmitting and receiving antenna. With respect to far-field measurements the distance of the positioners in the chamber determines the size of the antennas which can be measured [9]. With  $R$  the distance between the positioners,  $D$  the diameter of the antenna and  $\lambda$  the wavelength of the electromagnetic signal, the maximum diameter  $D$  of the antenna to be measured with respect to the wavelength is:

$$D \leq \sqrt{\frac{R\lambda}{2}} \quad (3.1)$$

Given a distance between the positioners of  $R = 3.5$  m, the maximum diameter  $D$  is 57.7 cm for the L1 frequency and 65.4 cm for the L2 frequency. This requirement meets the diameters of the antennas that were tested.

The set-up of the antenna measurements is as follows (see Figure 3.2): The column on which the Antenna Under Test (AUT) is placed has three degrees of freedom, translation in the  $x$ -direction (sideways), translation in the  $y$ -direction (towards antenna), and rotation around the  $z$ -axis. The column, on which the transmitting horn-antenna is placed, is fixed at its position. The rotation point of the receiving positioner is fixed at a distance of 3.5 m from the transmitting positioner. So the rotation point of the AUT can be chosen by

moving the column in x and y direction. The rotation point is the point where the measurements are referred to. The position of the phase center varies when the measurements are performed at different elevation angles, and so varies the measured phase. The variation of the measured phase is the elevation angle dependent phase center variation. When a minimum variation of the measured phase is found for a certain elevation-range of interest, the offsets (x,y) of the phase center are determined. The point at the rotation-axis represents the averaged phase center of the AUT.

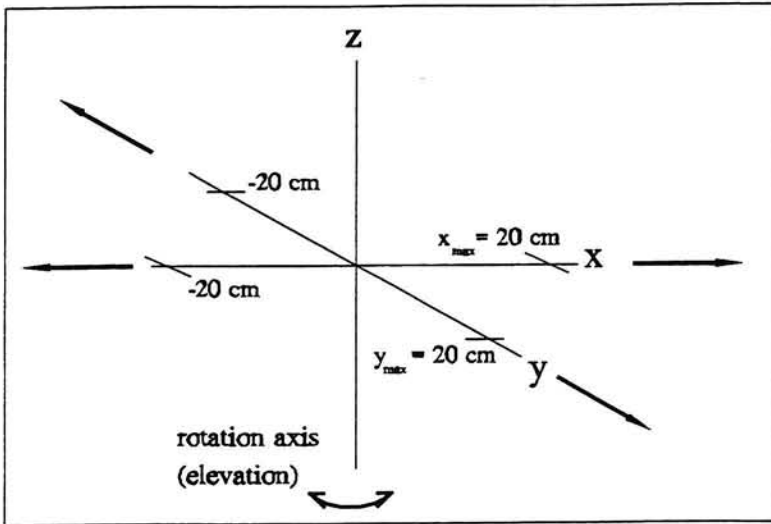
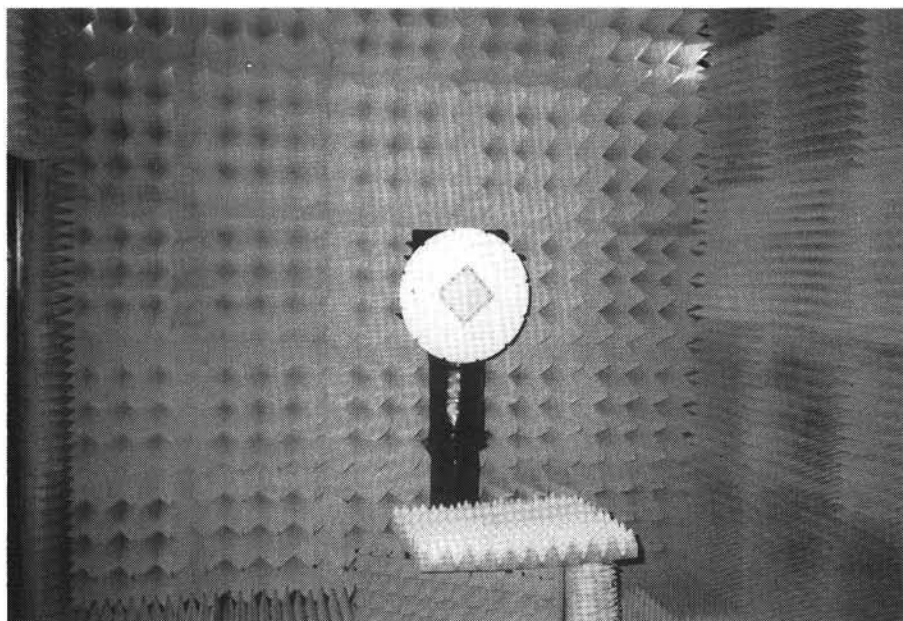


Figure 3.2: The receiving positioner can move in three directions.

The phase patterns are normalized during the measurements. Normalization means that the measured phase at zenith is set to zero. The normalized patterns show a phase center variation with respect to the determined averaged phase center. It is possible that there exists an offset between the averaged phase center and the apparent phase center at zenith, so the real pattern of the phase center is a translation of the pattern. This effect was not studied during the measurements.

The transmitting antenna and the AUT are aligned with a laser. The laser is placed on top of the column of the transmitting antenna and illuminates a small pin located on top of the column of the receiving positioner. The column of the receiving positioner rotates about the z-axis, while it is illuminated by the laser. If the light that strikes the small pin remains constant, it means that the column-axis with known (x,y) offsets coincide with the rotation axis. This means that the AUT and the transmitting antenna are well aligned.

More than 200 measurements were performed to determine the phase center characteristics of the tested antennas for L1 and L2. In the next section the results of the phase center measurements of the tested antennas, the Trimble 4000ST and the TurboRogue Dorne-Margolin, are given.



**Figure 3.3:** The Trimble antenna in DUCAT.

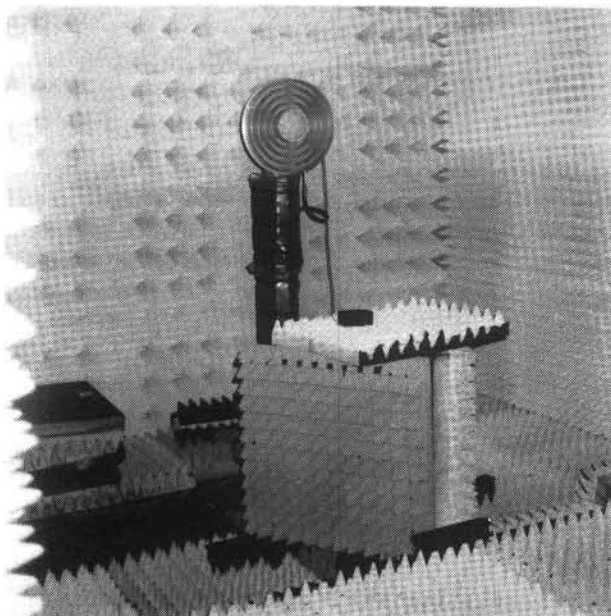


**Figure 3.4:** The TurboRogue antenna in DUCAT.

## 3.2 Results of phase center measurement

The Trimble antenna is, as discussed in section 2.4, a microstrip antenna type. The identity number of the tested Trimble antenna is 3249A66631. The minimum phase center variation is determined for the elevation-range of interest  $-75/75$  degrees. The TurboRogue antenna is, as discussed in section 2.4, a crossed dipole antenna type plus choke ring. Two different TurboRogues are tested, the identity numbers of the antennas are the T177 and T178. The determined phase center variations of the T177 are used for the processing of data with phase center corrections, discussed in chapter 4. The phase center variations of the T178 are determined to study if the results are the same as the T177. The minimum phase center variation is determined for the elevation-range of interest  $-75/75$  and  $-90/90$  degrees. The phase variation of the antennas are converted in a distance variation using the antenna delay function equation (2.1):

$$\Delta d(\theta, \phi) = \frac{c}{f} \Delta \Phi(\theta, \phi) \quad (3.2)$$

The phase center distance variations are used in chapter 4 for the correction of the processed data. Figures 3.3 and 3.4 show the Trimble and TurboRogue antenna in DUCAT.

As discussed in the previous chapter, a search is made to find a point in the AUT for which the phase variation of the phase center is minimized. Figure 3.5 shows the variation of the Trimble phase center for L1 at azimuth  $\phi = 180^\circ$  (South direction) as the column-axis is moved from  $y = 131$  mm (distance between column-axis and rotation axis) to 139, 153, 171 mm (this values correspond with a vertical averaged phase center of respectively, 5.6, 13.6, 27.6 and 45.6 mm measured from the front plane of the antenna). The offset  $y = 131$  mm corresponds with the upper pattern and  $y = 171$  mm with the lowest pattern. Notice that the phase variations are plotted as a function of zenith instead of elevation. During the measurement session more  $y$  values were measured, Figure 3.5 shows only a part of the results. The determination of the minimum phase shift variation is achieved when an elevation-range of interest is taken into account. The elevation-range of interest in Figure 3.5 is set at  $-75/75$  degrees. The phase pattern corresponding to  $y = 139$  mm gives the minimum phase shift of the phase center for this elevation-range. So the vertical L1 offset of the averaged phase center is 13.6 mm. From the measurements it is difficult to tell if the phase center variations for  $y = 138$  mm or 140 mm could represent the minimum phase center variations. But at the vicinity of the position where the phase center is found, the differences between the phase center patterns are very similar.

Figures 3.6 and 3.7 show the minimum L1 and L2 phase center variations for the Trimble antenna for elevation-range of interest  $-75/75$  degrees. The figures show the results at azimuth  $\phi = 180^\circ$  for respectively, L1 with vertical phase center offset 13.6 mm, L2 with

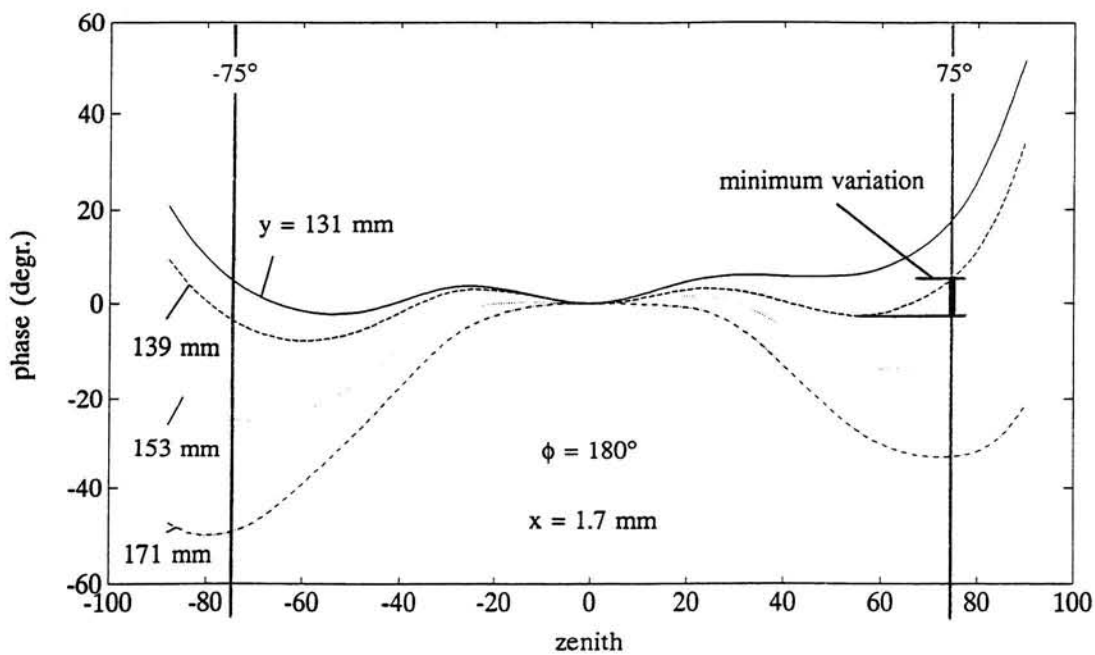


**Figure 3.5:** Determination of the L1 minimum phase center variation of the Trimble antenna for the elevation-range of interest  $-75/75$  degrees.

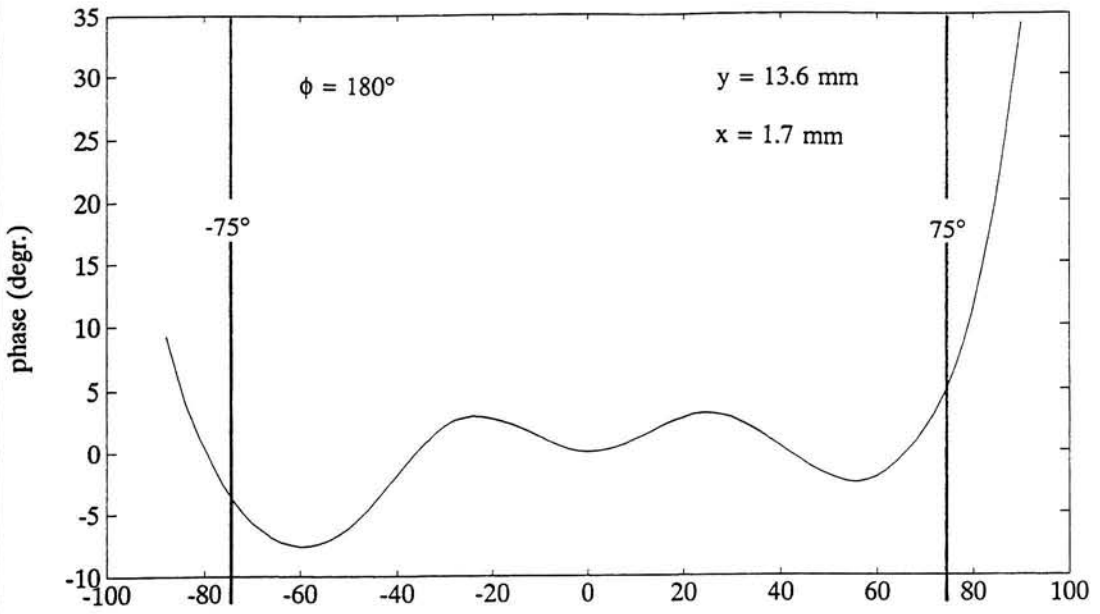


**Figure 3.6:** Minimum L1 phase center variation of the Trimble antenna for the elevation-range of interest  $-75/75$  degrees.

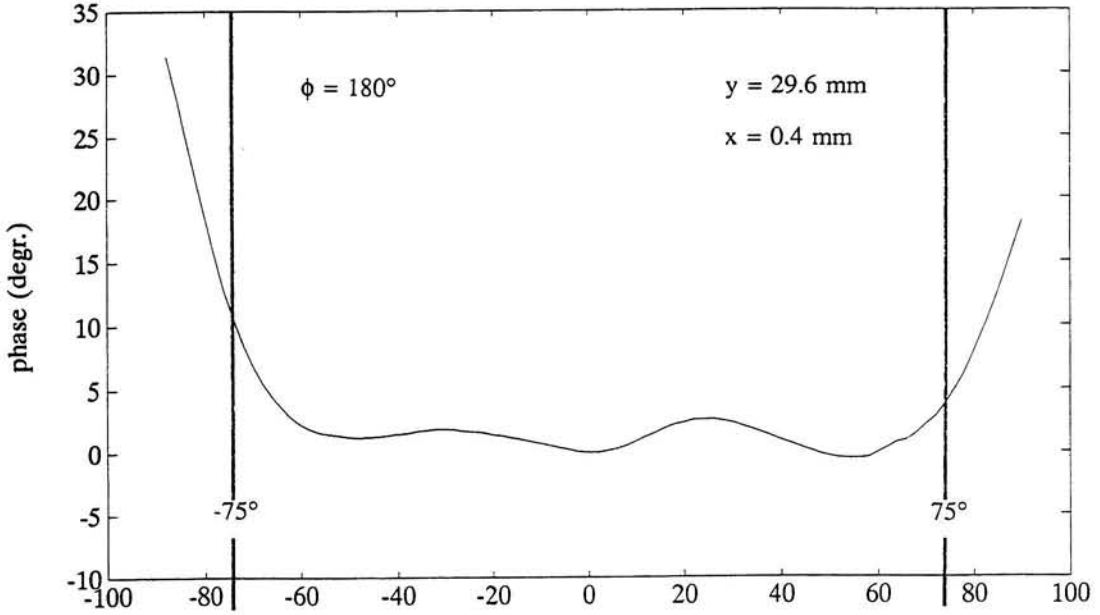


**Figure 3.7:** Minimum L2 phase center variation of the Trimble antenna for the elevation-range of interest  $-75/75$  degrees.

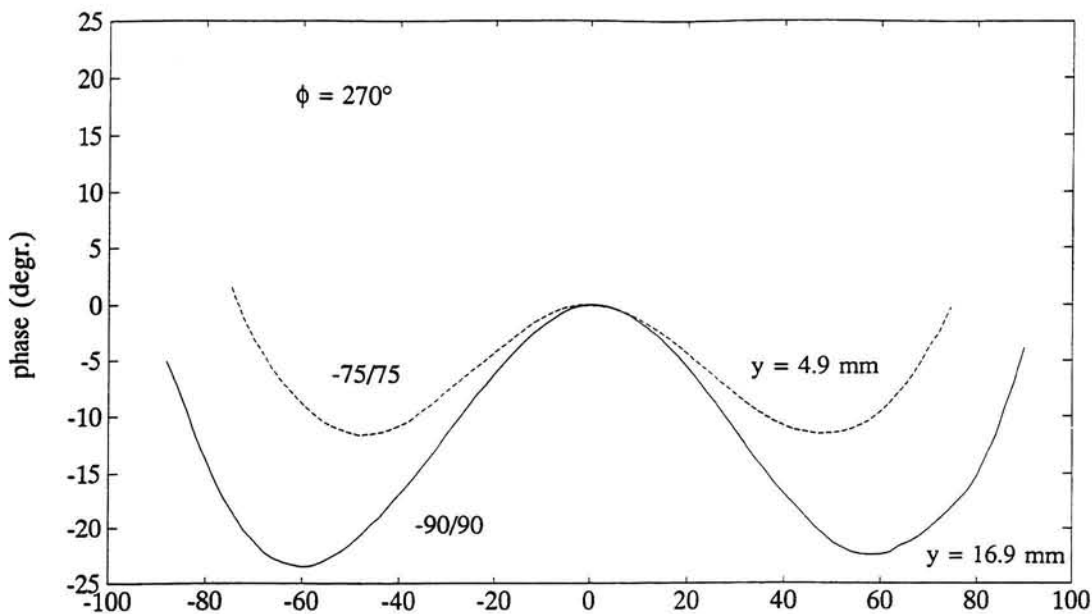


**Figure 3.8:** Minimum L1 phase center variation of the TurboRogue T177 antenna for the elevation-range of interest -75/75 and -90/90 degrees.

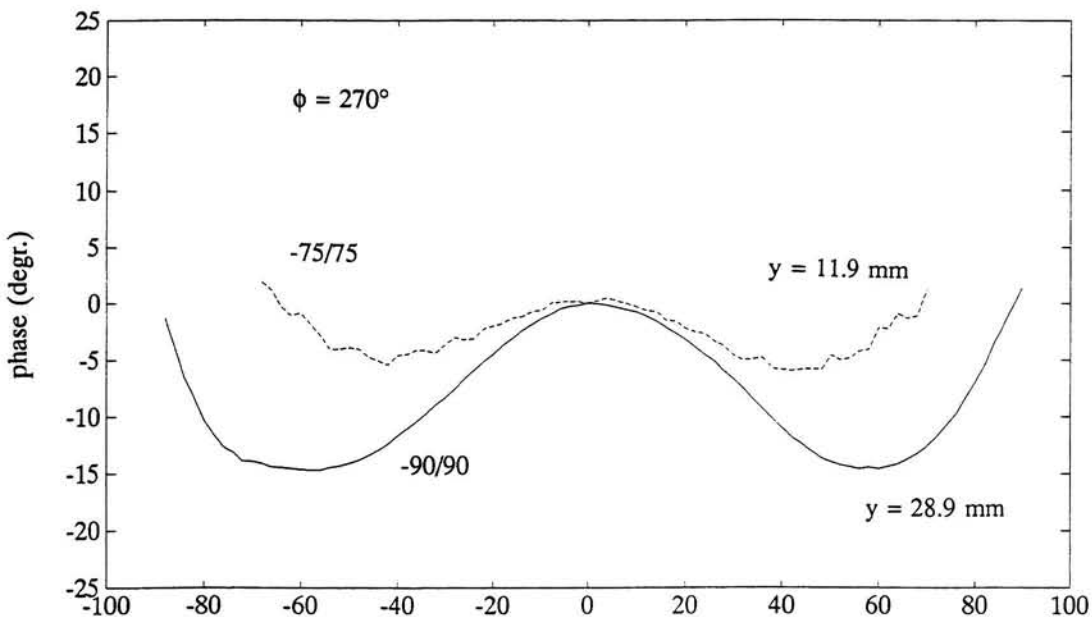


**Figure 3.9:** Minimum L2 phase center variation of the TurboRogue T177 antenna for the elevation-range of interest -75/75 and -90/90 degrees.

vertical phase center offset 29.6 mm. The vertical offset of the average phase center is measured from the front plane of the antenna. Both L1 and L2 show an asymmetry of the phase pattern between the positive and negative elevation angle region.

Figure 3.8 shows the minimum L1 phase center variations for the TurboRogue T177 antenna for the elevation-range of interest  $-75/75$  and  $-90/90$  degrees at  $\phi = 270^\circ$ . The vertical offsets of the average phase center are measured from the front plane of the antenna. For the elevation-range of interest  $-75/75$  degrees the vertical offset is found at 4.9 mm. For the elevation-range  $-90/90$  degrees the vertical offset is found at 16.9 mm. Figure 3.9 shows the minimum L2 phase center variation for the elevation-range of interest  $-75/75$  and  $-90/90$  degrees at  $\phi = 270^\circ$ . The vertical offset of the phase center for elevation-range  $-75/75$  degrees is found at 11.9 mm measured from the front plane of the antenna. For elevation-range  $-90/90$  degrees the vertical offset is found at 28.9 mm. The L2 pattern for elevation-range  $-75/75$  degrees shows a strange behavior. This behavior is probably caused by the frequency, because the L1 frequency does not show this problem. The shielding of the chamber can cause problems, since it is designed for frequencies above 2 GHz (see Table 3.1). The results show different minimum phase center variations and different phase center offsets for L1 and L2. Figures 3.8 and 3.9 show that it is important to consider the elevation range of interest, since for different elevations-ranges different phase center offsets and different minimum phase shift variations are found. From the results we can not conclude which phase patterns must be used for the processing of data.

Eight phase center measurements are performed as function of azimuth. The AUT is rotated in steps of  $45^\circ$  about the Y-axis (see Figure 3.2), and again rotated  $\pm 90^\circ$  about the elevation ( $\theta$ ) axis while recording the phase change. This operation is repeated for  $\phi$  equal to  $0^\circ, 90^\circ, 135^\circ, 180^\circ, 225^\circ, 270^\circ$  and  $315^\circ$ . Figures 3.10 and 3.11 show the L1 and L2 phase patterns for three azimuth directions for the Trimble antenna. The Trimble L1 patterns show small differences between the different azimuth directions, while the L2 patterns show larger variations. Both figures show an asymmetry of the phase patterns. Figures 3.12 and 3.13 show the L1 and L2 phase patterns for three azimuth directions for the TurboRogue T177 antenna. The figures show small differences between the different azimuth directions for the L1 and L2. Both figures show symmetry of the phase patterns. Comparing the L1 and L2 results of TurboRogue with the Trimble antenna, the figures show that the phase center variation of the Trimble antenna is more azimuth dependent than the TurboRogue antenna. The results shown in the Figures 3.10-3.13 can be illustrated in a three-dimensional shape, see Figure 3.14.

The horizontal phase center offsets  $x$  are determined for the best symmetrical phase pattern. Tables 3.2 and 3.3 give the horizontal offsets for L1 and L2 for the different azimuth directions for respectively, the Trimble antenna and the TurboRogue T177 antenna. The variation of the horizontal offset is larger in L2 than L1 for both antennas. The Trimble offsets show larger variations compared with TurboRogue. The TurboRogue L1 horizontal offset show small variations, the phase center is located near the physical center of the antenna. These results show that the horizontal offset of the Trimble antenna is more azimuth dependent than the TurboRogue antenna.

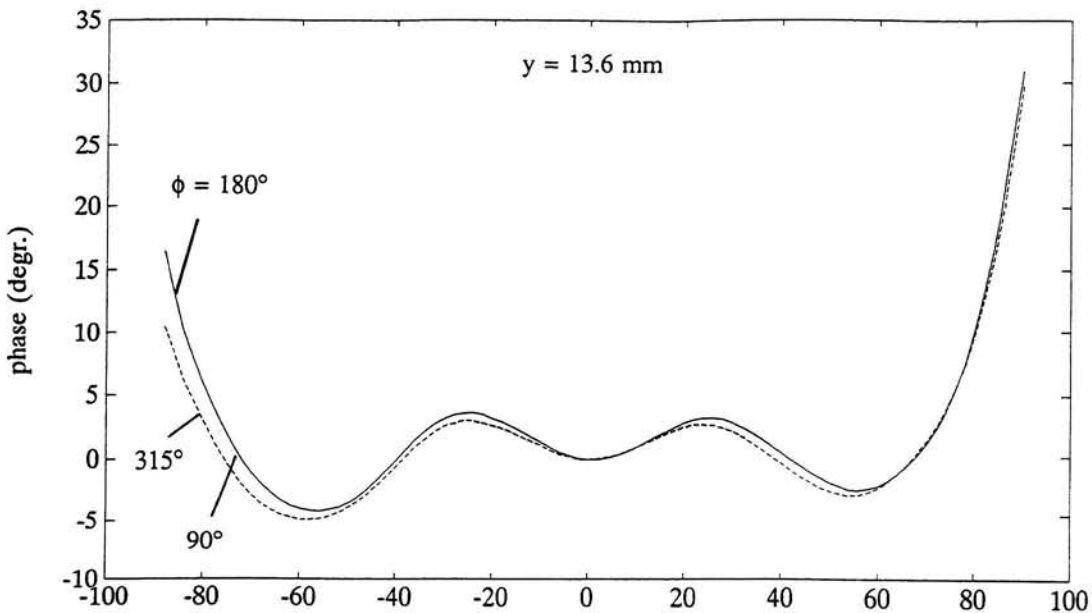


**Figure 3.10:** Minimum L1 phase center variation of the Trimble antenna for 3 different azimuth directions for the elevation-range of interest -75/75 degrees.

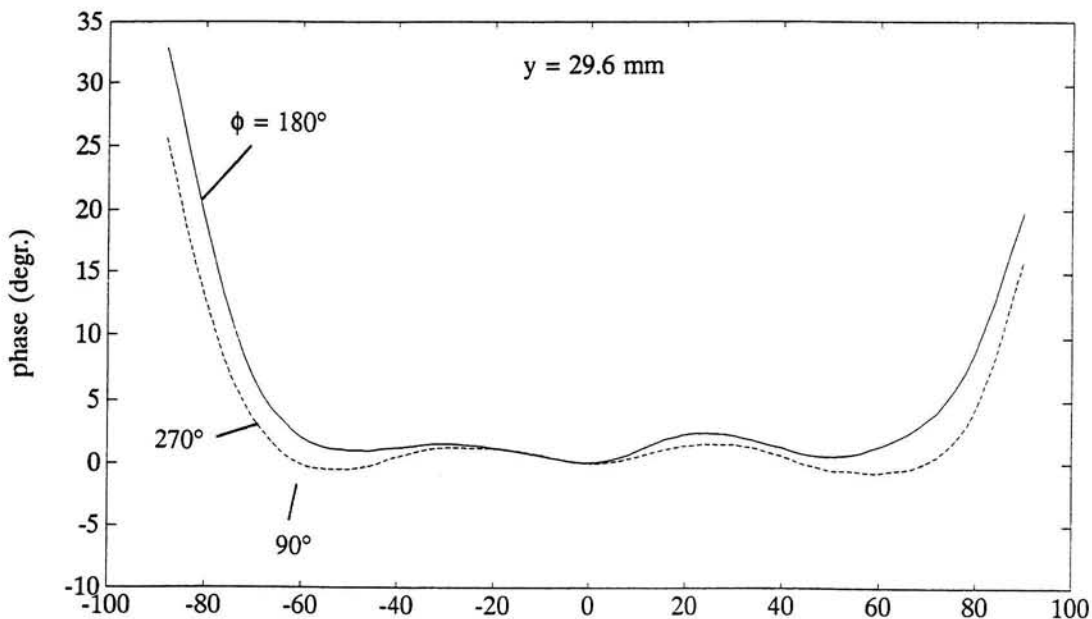


**Figure 3.11:** Minimum L2 phase center variation of the Trimble antenna for 3 different azimuth directions for the elevation-range of interest -75/75 degrees.

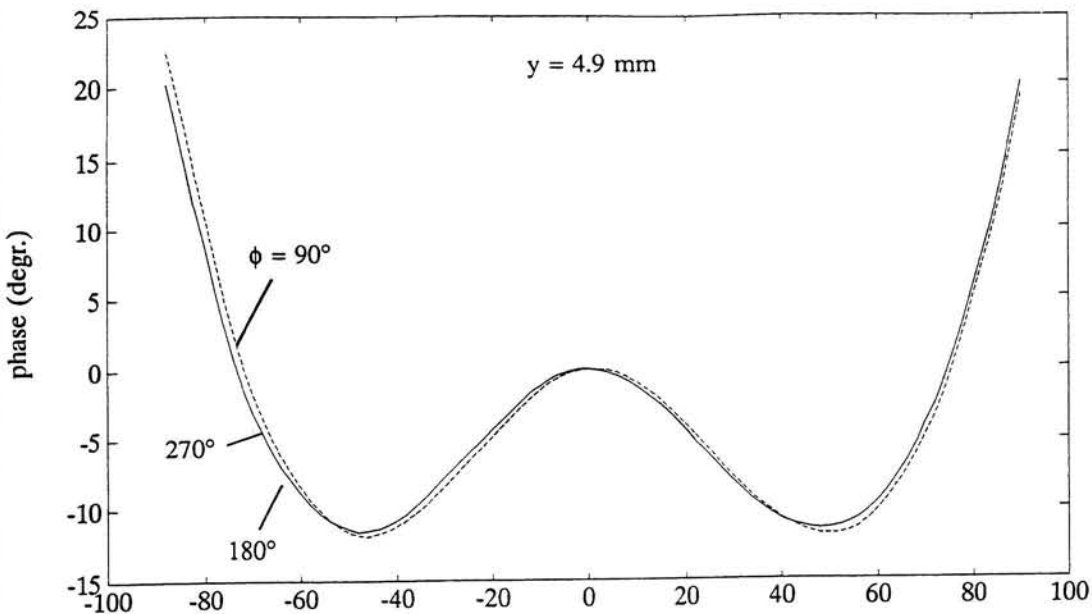


**Figure 3.12:** Minimum L1 phase center variation of the TurboRogue T177 antenna for 3 different azimuth directions for the elevation-range of interest -75/75 degrees.

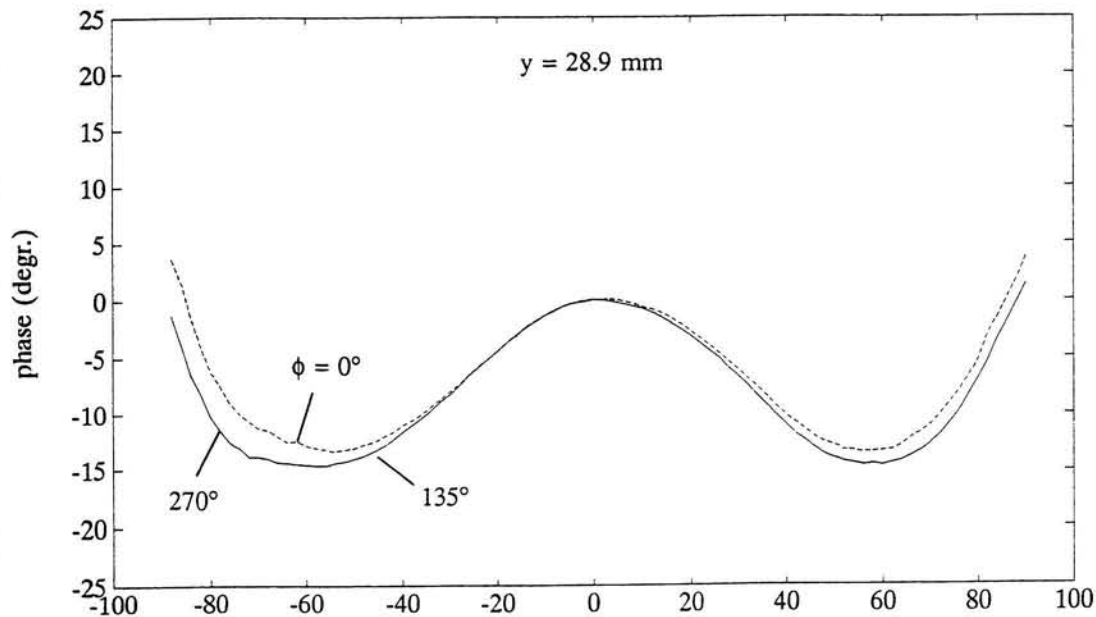


**Figure 3.13:** Minimum L2 phase center variation of the TurboRogue T177 antenna for 3 different azimuth directions for the elevation-range of interest -90/90 degrees.

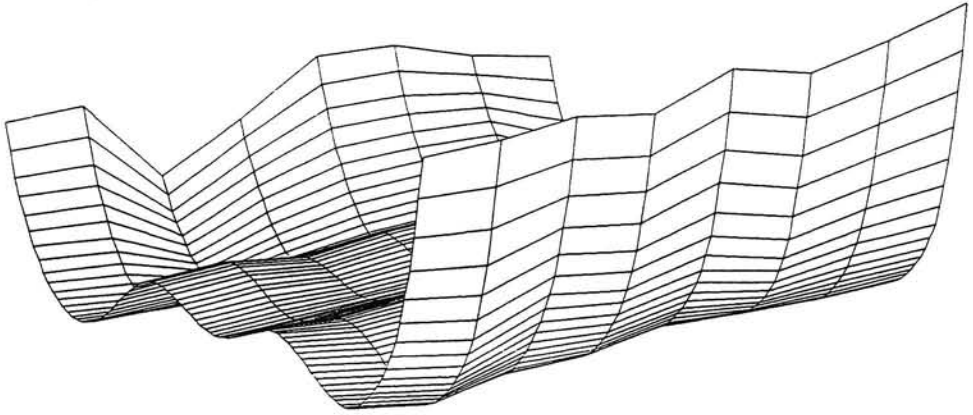


**Figure 3.14a:** Trimble L1 phase center variation as function of elevation and azimuth.

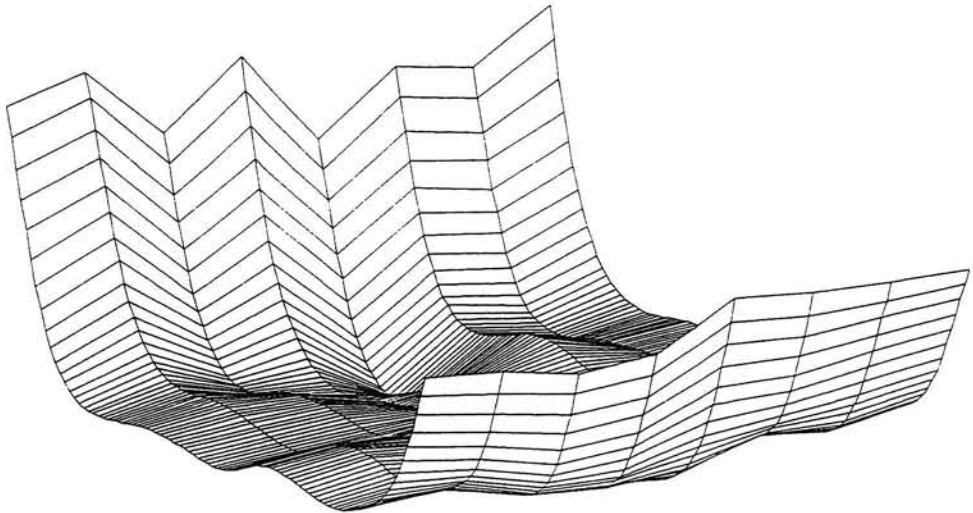
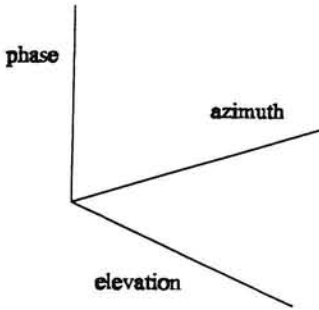


**Figure 3.14b:** Trimble L2 phase center variation as function of elevation and azimuth.

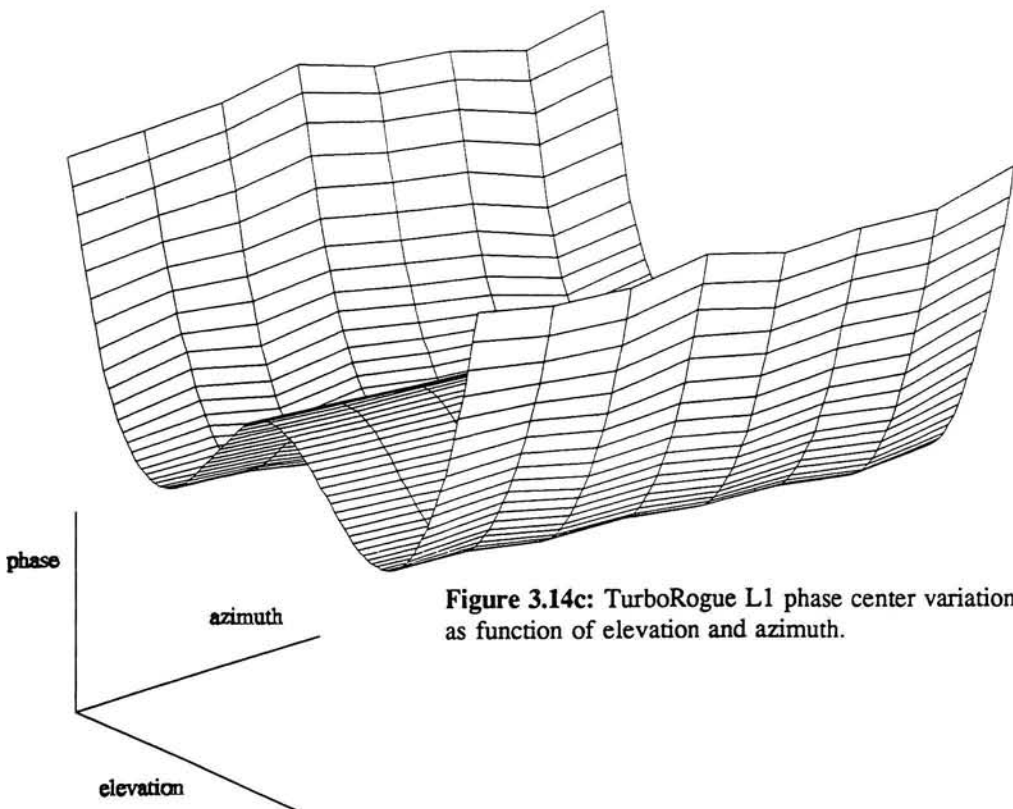


**Figure 3.14c:** TurboRogue L1 phase center variation as function of elevation and azimuth.

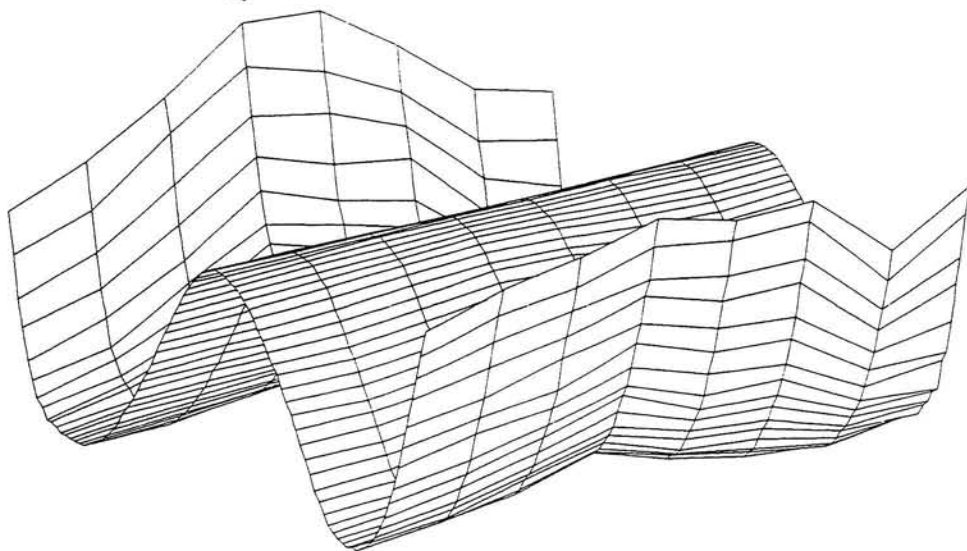


**Figure 3.14d:** TurboRogue L2 phase center variation as function of elevation and azimuth.

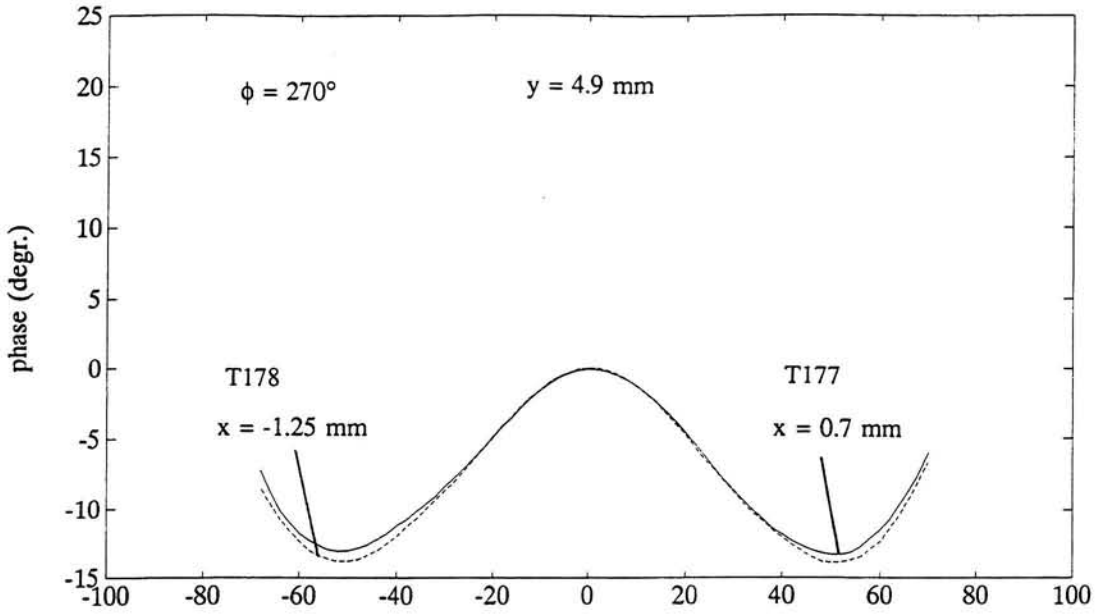


**Figure 3.15:** Minimum L1 phase center variation of the TurboRogue T177 and T178 for the elevation-range of interest -75/75 degrees.

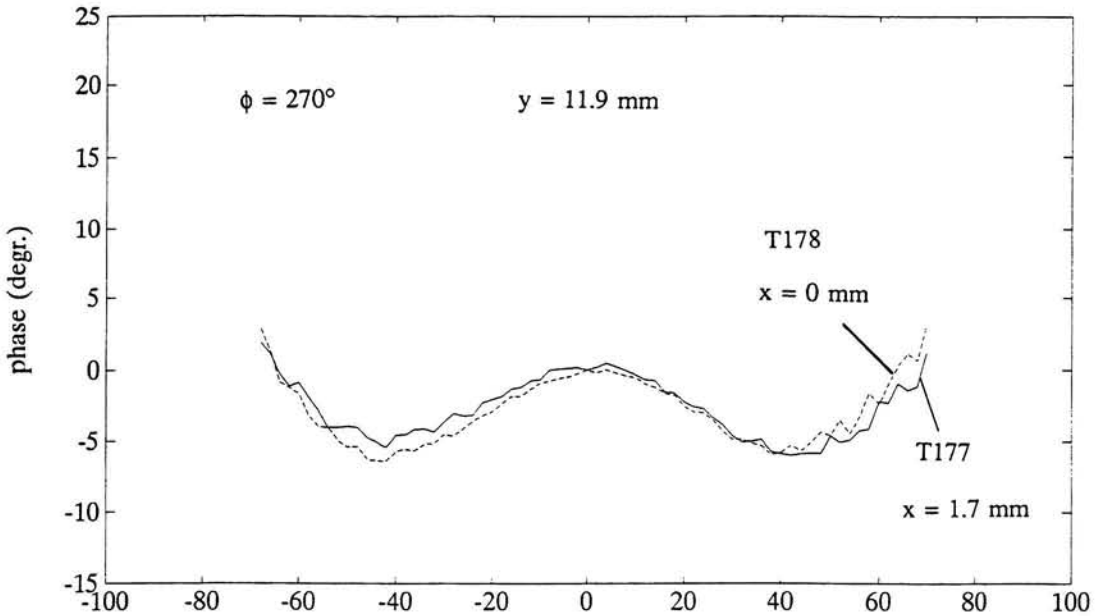


**Figure 3.16:** Minimum L2 phase center variation of the TurboRogue T177 and T178 for the elevation-range of interest -75/75 degrees.

**Table 3.2:** Horizontal L1 and L2 phase center offsets for the Trimble antenna.

azimuth $\phi$ (degr)	horizontal offset x (mm)		azimuth $\phi$ (degr)	horizontal offset x (mm)	
	L1	L2		L1	L2
0 (North)	-2.0	-4.8	180	1.7	0.4
45	-1.7	-7.0	225	-0.6	1.2
90	-1.9	-7.2	270	-0.5	1.5
135	-1.2	-3.7	315	0.5	0.8

**Table 3.3:** Horizontal L1 and L2 phase center offsets for the TurboRogue T177 antenna.

azimuth $\phi$ (degr)	horizontal offset x (mm)		azimuth $\phi$ (degr)	horizontal offset x (mm)	
	L1	L2		L1	L2
0 (North)	1.3	2.6	180	0.5	2.4
45	2.1	4.9	225	0.8	2.3
90	1.8	4.0	270	0.7	1.7
135	0.6	1.8	315	0.5	1.9

The objective of measuring the TurboRogue T178 is to examine if both antennas (T177 and T178) show the same phase center characteristics. Only one azimuth direction is measured. The phase center offset and variation are determined for elevation-range of interest  $-75/75$  degrees. For this elevation-range a vertical phase center offset is found of 4.9 mm for L1 and an offset of 11.9 mm for L2 for the T177 antenna. These values were introduced for the T178 and the results are shown in Figure 3.15 for L1 and Figure 3.16 for L2. The figures show small differences between T178 and T177 for L1 and L2. The negative maximum of the L1 T178 pattern is a little bit larger than the maximum of the T177. Despite of the strange behavior of the L2 phase pattern, a difference in the symmetry of the pattern can be seen. So between TurboRogue antennas small differences in the phase center characteristics exist, but these small differences can also be caused by the conditions of the chamber. Temperature and mechanical action can influence the measurements, resulting in different phase center offset and phase center variation. So it does not mean that both TurboRogues are two different antennas since the differences of the phase patterns are not different enough as is the case between the TurboRogue and Trimble antenna.

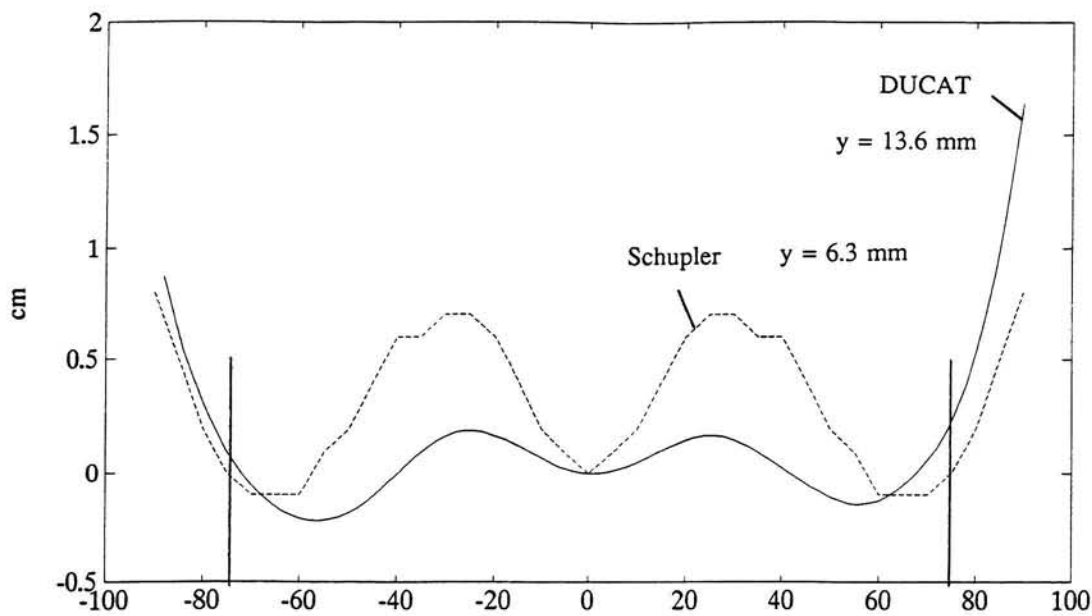


**Figure 3.17:** Trimble L1 phase center variation; comparison between DUCAT (elevation-range -75/75 degrees) and Schupler (elevation-range -90/90 degrees).

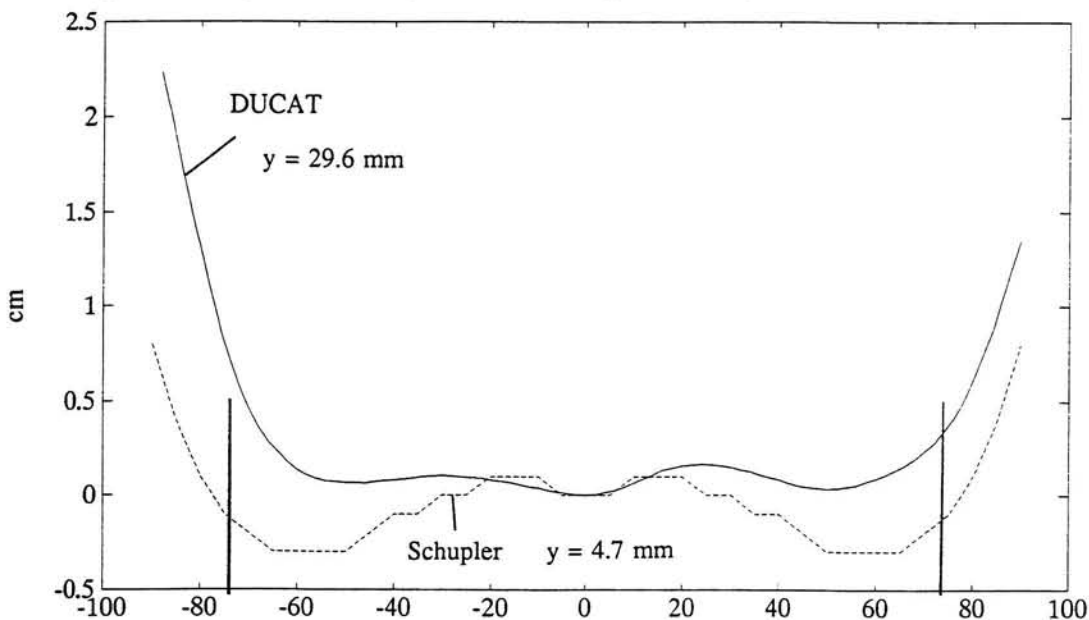


**Figure 3.18:** Trimble L2 phase center variation; comparison between DUCAT (elevation-range -75/75 degrees) and Schupler (elevation-range -90/90 degrees).

In this section we have shown that there is a clear and significant elevation dependence at both frequencies for the Trimble and TurboRogue antenna. The phase patterns of the Trimble and TurboRogue are different. Between the T177 and T178 TurboRogue antenna the differences in the phase pattern are roughly the same. The question remains if these differences are significantly different, so that we can speak about two different antennas. An other important aspect is the elevation-range of interest. Different minimum phase shift variations are found for different elevation ranges. Therefore, the minimum phase center variation of the phase center can not be determined uniquely.

### 3.3 Comparison with former phase center measurements

Schupler et al. [11] determined elevation angle and azimuth angle dependent phase center variations for the Rogue and Trimble antennas. They provide averaged phase centers over different azimuth directions. These averaged phase center variations depend only on the elevation-range of interest  $-90/90$  degrees.

The results of the Trimble phase center variations measured at DUCAT are compared with the results of Schupler. Figure 3.17 shows the L1 phase pattern comparison. The patterns are for the azimuth North direction of the antenna. The patterns are significant different. The phase pattern determined at DUCAT shows a smaller phase shift variation when an elevation-range of interest of  $-75/75$  degrees is considered. But the phase pattern of Schupler shows a smaller phase shift variation for the elevation-range of interest of  $-90/90$  degrees. Figure 3.18 shows the Schupler and DUCAT phase center variation for the L2. Comparison of both patterns show also differences, but they are smaller when compared with the L1 patterns. The DUCAT phase pattern shows a smaller phase shift variation for the elevation-range  $-75/75$ , but a larger phase shift variation for elevation-range  $-90/90$ . The figures show that different elevation-ranges of interest causes different minimum phase center variations. The determined averaged vertical phase center offsets of Schupler and DUCAT differ for L1 as for L2. The phase center offsets are given in Table 3.4.

The TurboRogue phase center variations measured at DUCAT for elevation-range of interest  $-90/90$  degrees are compared with the results of the Rogue measured by Schupler. Figures 3.19 and 3.20 show the L1 and L2 phase pattern comparison. The patterns are for the azimuth North direction of the antenna. The L1 phase center variation of the TurboRogue show a different pattern when compared with the L1 phase center variation of the Rogue. The Rogue phase center variation is also determined for the elevation-range  $-90/90$  degrees. It can be seen that there exist differences between TurboRogue and Rogue. But as is the case between TurboRogue T177 and T178 (see section 3.2): are these differences different enough to conclude that TurboRogue and Rogue are two different antennas? The L2 phase center variation of the TurboRogue and the L2 phase center variation of the Rogue, both for elevation-range of interest  $-90/90$  degrees, are almost identical. The determined vertical phase center offsets of the TurboRogue are given in Table 3.5.

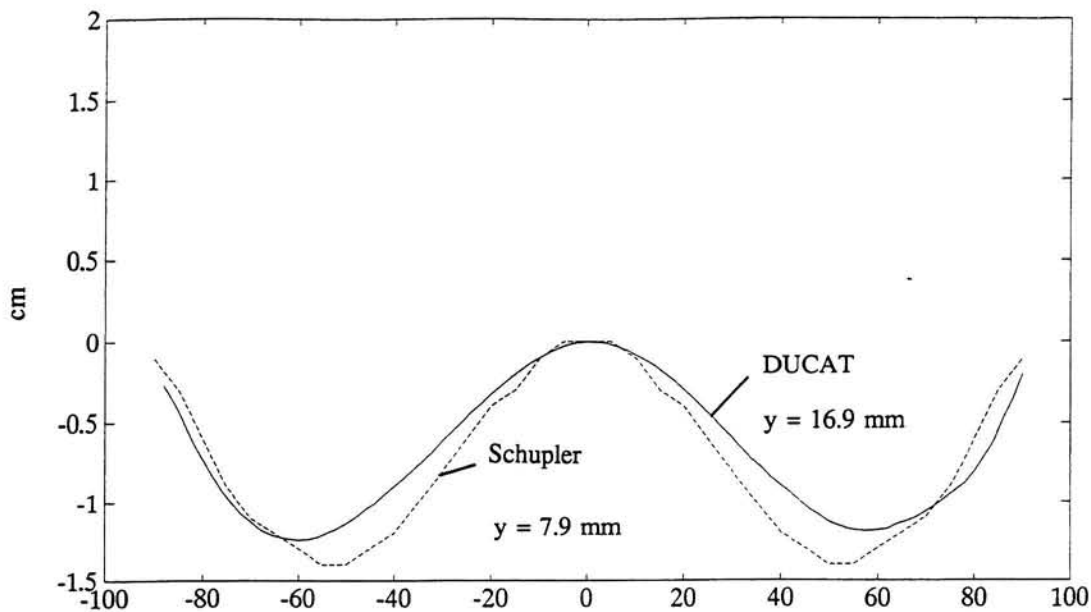


**Figure 3.19:** Comparison between L1 phase center variation DUCAT (TurboRogue) and Schupler (Rogue), both for the elevation-range of interest -90/90 degrees.

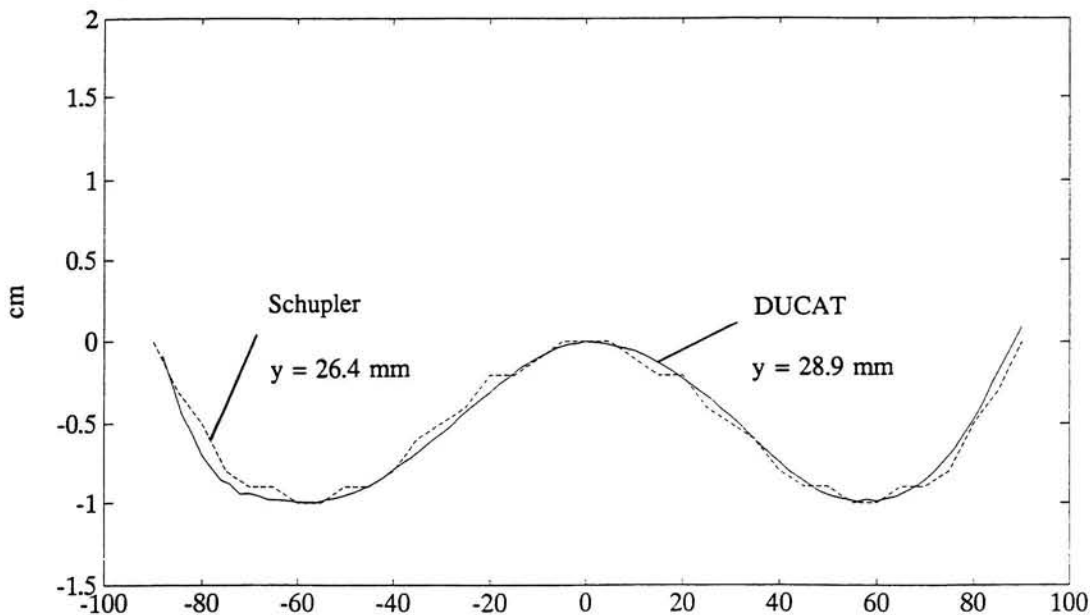


**Figure 3.20:** Comparison between L2 phase center variation DUCAT (TurboRogue) and Schupler (Rogue), both for the elevation-range of interest -90/90 degrees.

ESTEC [13] determined also phase center variations for the Rogue antenna. The L1 and L2 phase patterns of the Rogue measured by ESTEC are compared with the phase patterns of the Rogue measured by Schupler. Figures 3.21 and 3.22 show the different patterns. As is the case with the Trimble and TurboRogue antenna, different minimum phase shift variations of the pattern are found when the elevation-range of interest is taken into account. The ESTEC phase patterns for both frequencies show a minimum phase shift variation when an elevation-range of interest of  $-75/75$  degrees is taken into account. The Schupler phase patterns for both frequencies have a minimum phase shift variation when an elevation-range of  $-90/90$  degrees is taken into account. The vertical phase center offsets are given in Table 3.6.

**Table 3.4:** Vertical L1, L2 and L3 phase center offsets Trimble antenna.

	Schupler (m)	DUCAT $-75/75$ degrees (m)
L1	.0063	.0136
L2	.0047	.0296
L3	.0088	-.0111

**Table 3.5:** Vertical L1, L2 and L3 phase center offsets TurboRogue antenna.

	DUCAT $-75/75$ degrees (m)	DUCAT $-90/90$ degrees (m)
L1	.0049	.0169
L2	.0119	.0289
L3	-.0059	-.0017

**Table 3.6:** Vertical L1, L2 and L3 phase center offsets Rogue antenna.

	Schupler (m)	ESTEC (m)
L1	.0079	.0069
L2	.0264	.0305
L3	-.0207	-.0296

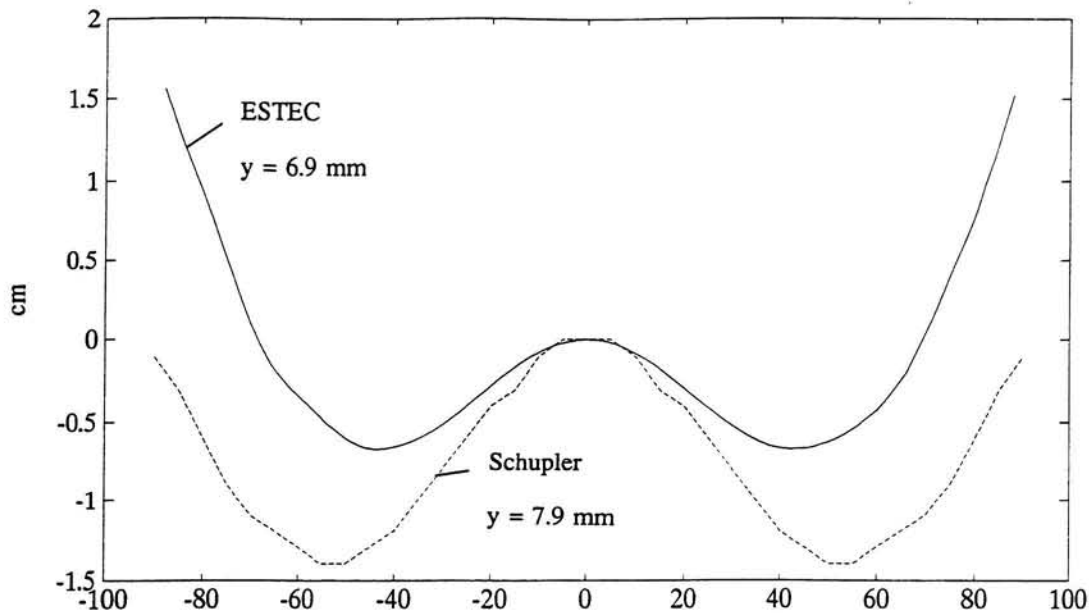


**Figure 3.21:** Rogue L1 phase center variation; comparison between ESTEC (elevation-range -75/75 degrees) and Schupler (elevation-range -90/90 degrees).

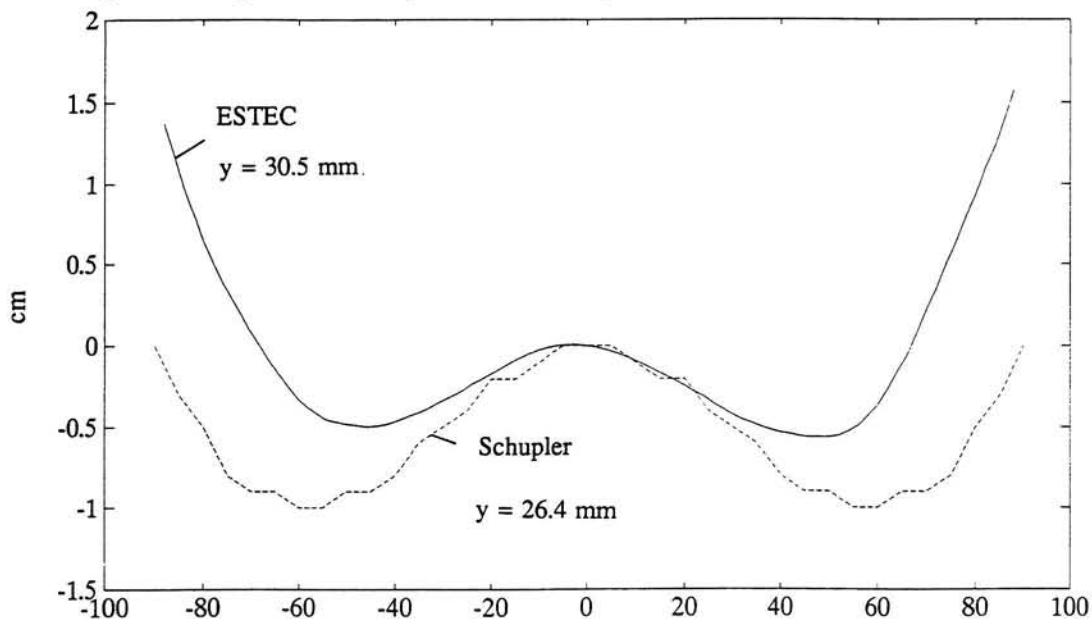


**Figure 3.22:** Rogue L2 phase center variation; comparison between ESTEC (elevation-range -75/75 degrees) and Schupler (elevation-range -90/90 degrees).

The L1 and L2 phase patterns of the TurboRogue T177 and T178 are compared with the phase patterns of the Rogue measured by ESTEC. Figures 3.23 and 3.24 show the different phase patterns. The patterns provide minimum phase shift variation for the elevation-range -75/75 degrees. For this elevation-range, the patterns show small differences between TurboRogue and Rogue, as is the case between TurboRogue and Rogue for elevation-range of interest -90/90 degrees. The differences between the different TurboRogues are smaller than the differences between TurboRogues and Rogue.

We have shown above that the tested TurboRogue, Rogue and Trimble antennas show different elevation and azimuth phase center variations for both frequencies. These differences can be caused by the following possibilities:

- Antennas of the same type are not identical, resulting in a different phase center offset and phase center variation.
- The minimum phase center variation depends on the elevation-range of interest.
- The conditions of the different chambers where the measurements of Schupler, ESTEC and DUCAT are performed, can influence the measurements, resulting in different phase center location and variation. The conditions of the chamber can be influenced by several factors: the temperature in the chamber, shielding of the chamber and set-up of the measurements. Also mechanical action can influence the measurements.

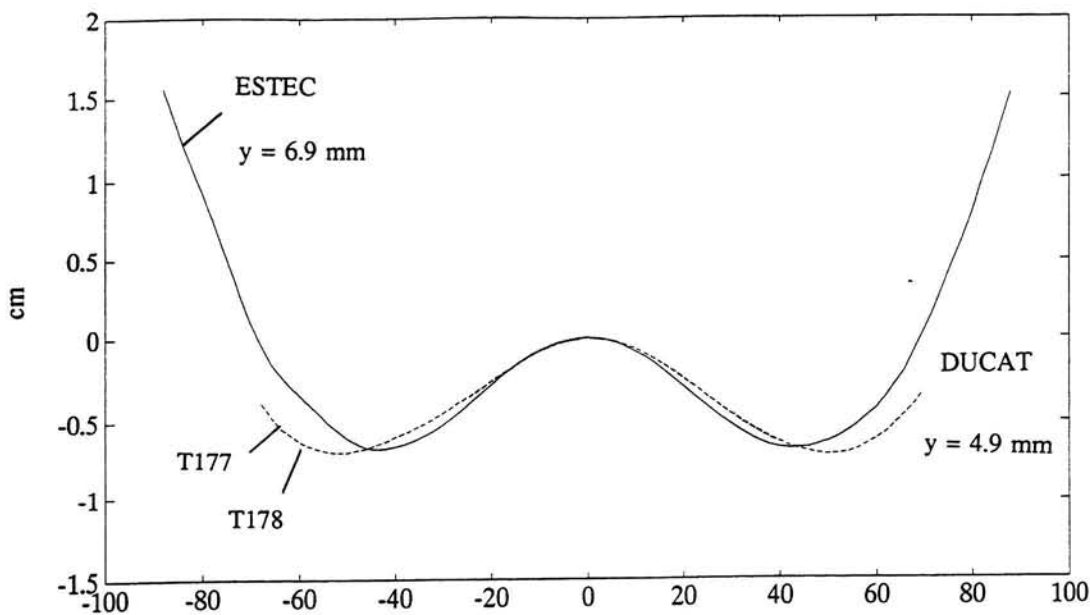


**Figure 3.23:** Comparison between L1 phase center variation DUCAT (TurboRogues T177 and T178) and ESTEC (Rogue), both for elevation-range of interest  $-75/75$  degrees.

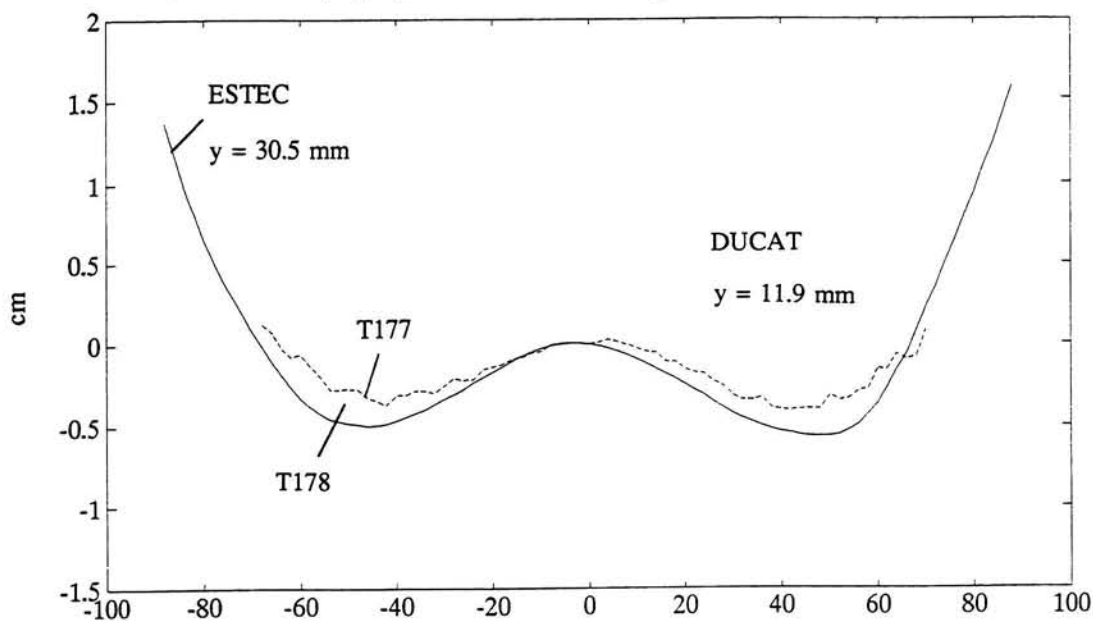


**Figure 3.24:** Comparison between L2 phase center variation DUCAT (TurboRogues T177 and T178) and ESTEC (Rogue), both for elevation-range of interest  $-75/75$  degrees.

## 4. Baseline results with different antennas

### 4.1 Introduction

The GPS data were collected in a measurement campaign in Delft and in Kootwijk from 10 to 14 May 1993. During this campaign seven GPS receivers were used. Three receivers were located at Delft and four in Kootwijk.

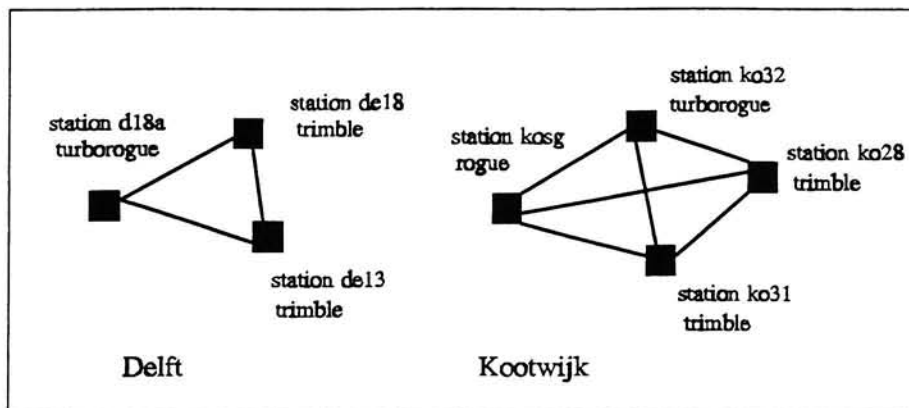
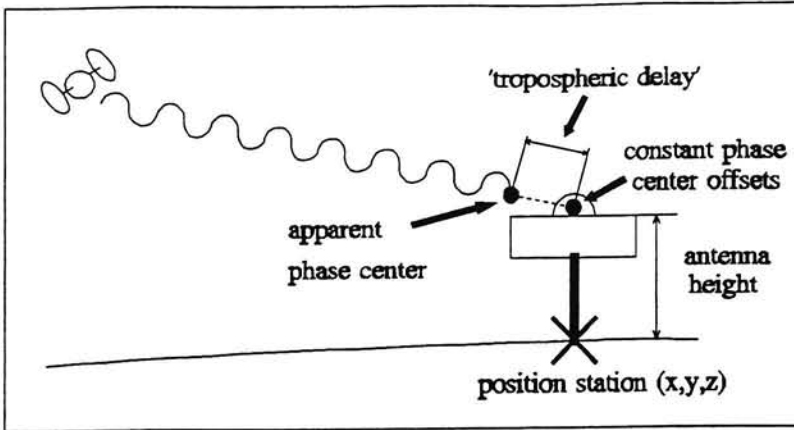


Figure 4.1: Network of stations in Delft and Kootwijk.

A network is defined consisting of different baselines between the receivers (stations). Two networks are studied in this report, see Figure 4.1. One network includes the baselines between the stations in Delft. The other network includes the baselines between the stations in Kootwijk. Both networks consist of short baselines (100 meters or less). The advantage of short baselines is the small influences of satellite orbits, ionosphere and especially the troposphere. The tropospheric influences should be (almost) identical for all stations in the small networks. Therefore, baseline results determined without tropospheric parameter estimation can be compared with the baseline results obtained with tropospheric parameter estimation, where we expect the results to be significantly different when different antennas are involved. The advantage of comparing these results, is because the difference between the two solutions will primarily be caused by the elevation dependent phase center variations. Other specific antenna values that are introduced in the software as phase center offsets, antenna height and site-tie vector remain constant. The software interprets the elevation dependent phase center variations as a tropospheric delay when the troposphere is estimated by a model (see equation 1.1). This results in a different solution of the baseline, see Figure 4.2.



**Figure 4.2:** Interpretation of the phase center as a tropospheric delay.

A network including all Delft and Kootwijk stations has not been chosen, because the distance between Delft and Kootwijk is too long (100 km) to neglect the tropospheric influences. So comparison between the baseline results with and without tropospheric parameter estimation is not meaningful. Table 4.1 gives the stations with the corresponding receivers and antennas. The Trimble SSE and SST receivers use the same Trimble 4000ST antenna. The antennas of the TurboRogue and Rogue receivers are of the same type but geometrical different of shape (see section 2.4).

**Table 4.1:** The Kootwijk and Delft stations with corresponding antennas.

station	receiver	antenna
KOSG	Rogue	Dorne-Margolin B
KO32	TurboRogue	Dorne-Margolin T
KO28	Trimble SSE	Trimble 4000ST
KO31	Trimble SST	Trimble 4000ST
D18A	TurboRogue	Dorne-Margolin T
DE13	Trimble SST	Trimble 4000ST
DE18	Trimble SSE	Trimble 4000ST

In this study we are mainly concerned in the vertical (height) component of the baseline. Solutions are obtained for L1 and L2, as for the L1/L2 combination, that is, the ionospheric free linear combination L3. Baselines are estimated for all combinations of stations that are possible for that specific day. The Delft-network includes all three stations for all

5 days. The Kootwijk-network includes station KOSG and KO28 for day 130, station KOSG, KO28, KO31 and KO32 for the days 131 and 132, and station KO28, KO31 and KO32 for the days 133 and 134.

The GPS data is processed with the GIPSY-OASIS II software package and the coordinate system used is WGS-84. First, satellite ephemerides are transformed into J2000 Earth-Centered-Inertial frame using precession, nutation, UT1 and polar motion. Next a fit is performed to find initial conditions consistent with the ephemerides. One orbit file is created for each satellite. The individual orbit files are combined into one final orbit. Individual data files are edited and decimated in samples of 6 minutes. None of the a priori station coordinates are fixed, the a priori sigmas are set at 1 meter. The clocks of the TurboRogue receivers D18A (for Delft) and KO32 (for Kootwijk) are used as reference clocks. For day 130 (Kootwijk) the Rogue clock (KOSG) is used as reference clock. Additional information that is not provided by the receivers, e.g. antenna height, antenna phase center offsets, angle dependent phase center variations and approximate station coordinates have to be introduced in the software. During the processing of the data, estimation of the baseline solutions with the code observations for the L1 and L2 signals produced some difficulties. This was due to the opposite sign of the ionospheric influence for the phase and code measurements. Only processing of the phase observations was possible. The processing of the code and phase observations of the L3 signal caused no problems. To minimize the influence of atmospheric errors at low elevations, the cut-off elevation was set at 15 degrees. Notice that for all processed results the only variable in this study is the estimation of the troposphere. The troposphere is estimated as a random walk process with an a priori sigma of 0.5 meter for the estimated delay and an a priori sigma of  $1 \text{ cm}/\sqrt{\text{h}}$  for the random walk process.

In the next section the results of the processed baselines with different antennas are given. Furthermore, results obtained during the IGS campaign at CODE (Center of Orbit Determination Europe) and results obtained by UNAVCO are given. Finally, the results are discussed.

## 4.2 Mixed-baseline results

When discussing the results of the estimated baselines with or without tropospheric parameter estimation, two things must be distinguished: (a) The offsets of the L1, L2 and L3 solutions without tropospheric parameter estimation (NoTrop) and with tropospheric parameter estimation (TropEst), (b) and the difference between the NoTrop and TropEst solutions for L1, L2 and L3. In this study we are mainly interested in the difference between the NoTrop and TropEst solution for L1, L2 and L3. The offsets for L1, L2 and L3 solutions can be corrected by introducing constant phase center offsets in the software. Furthermore, only the height-solutions of the baselines are determined. The following figures show only the difference between NoTrop and TropEst.

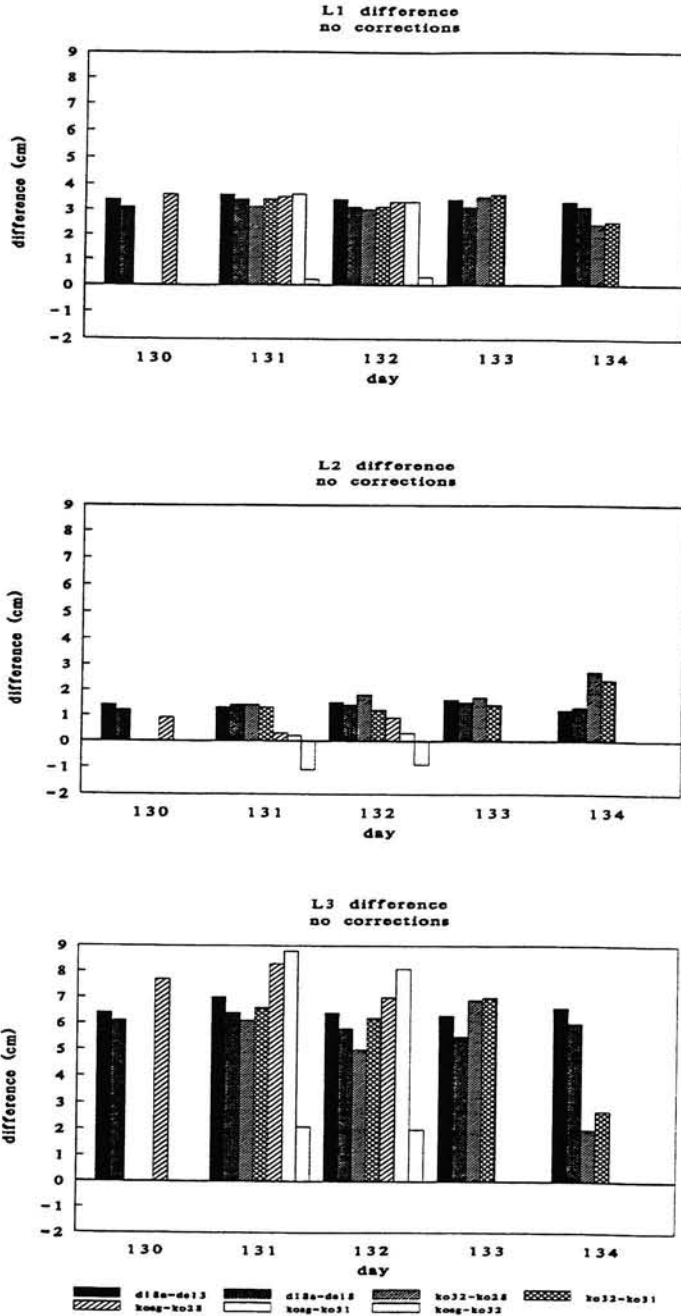


Figure 4.3a: Vertical mixed-baseline results with no corrections applied.

Figure 4.3a shows the height-differences between NoTrop and TropEst L1, L2 and L3 solutions for mixed-baselines without phase center corrections. These figures need some explanation: The first two bars represent the difference (in centimeters) between Notrop and TropEst for the Delft TurboRogue-Trimble baselines (D18A-DE13 and D18A-DE18). The following two bars represent the difference for the Kootwijk TurboRogue-Trimble baselines (KO32-KO28 and KO32-KO31). The next two bars represent the difference for the Kootwijk Rogue-Trimble baselines (KOSG-KO28 and KOSG-KO31), and finally, the last bar represents the difference for the Rogue-TurboRogue baseline (KOSG-KO32). Notice that for day 130 no Kootwijk-baseline results are given (except baseline KOSG-KO28), because for this day no KO31 and KO32 data was available. For day 133 and day 134 no KOSG data was available, so no solutions for baselines including this station can be given. Figure 4.3a shows a significant difference between NoTrop and TropEst in L1, L2 and L3 for the TurboRogue-Trimble and Rogue-Trimble baselines. The difference between NoTrop and TropEst when different antennas are applied is more affected in L1 than L2. The differences between NoTrop and TropEst for the mixed TurboRogue-Trimble (TR-T) and Rogue-Trimble (R-T) baselines are larger than the Rogue-TurboRogue (R-TR) baseline. Day 134 (Kootwijk) does not show the same difference in L1, L2 and L3 as the other days. The R-TR baseline results show different solutions when NoTrop is compared with TropEst. The differences have positive and negative values. The difference between NoTrop and TropEst is about 2 cm for L3 and -1 cm for L2. The L1 difference is at sub-centimeter level, but opposite of sign with respect to the L2 difference. The results indicate that between TurboRogue and Rogue different phase center characteristics may exist. But as mentioned in the previous chapter the question still remains if these results are significantly different, so that we can conclude that both antennas are different. The TR-T and R-T baseline results show a much clearer difference when compared with the R-TR baseline. As shown above, mixing of the Trimble antenna with TurboRogue or Rogue antenna can lead to significant differences if troposphere parameters are estimated. Figure 4.3b shows the non-mixed Trimble-Trimble baseline L1, L2 and L3 height-differences between NoTrop and TropEst without phase center corrections. The figure shows that for L1, L2 and L3 the differences are very small. So between Trimble antennas the phase center variations seem to be the same.

To process the data with phase center corrections the results of the phase patterns given in chapter 3 are implemented in the software. We have shown in chapter 3 that different phase center offsets and phase center variations are found between the different antennas and between antennas of the same type for L1 and L2. Different phase center offsets and minimum phase center variations are found when the elevation-range of interest is considered (elevation range of  $-75/75$  and  $-90/90$  degrees). In this section the baseline results of the processed data with different combinations of the phase center corrections for each different antenna are given. The results are discussed in section 4.4.

The L1 and L2 phase center variations of the Trimble and the TurboRogue antenna determined in the chamber DUCAT, see Figures 3.6-3.7 (Trimble) and Figures 3.8-3.9 (TurboRogue), are introduced in GIPSY. For this combination the elevation-range of interest for the Trimble and TurboRogue antenna is  $-75/75$  degrees. For the Rogue antenna the L1 and L2 phase center variations determined by Schupler are introduced (see Figures

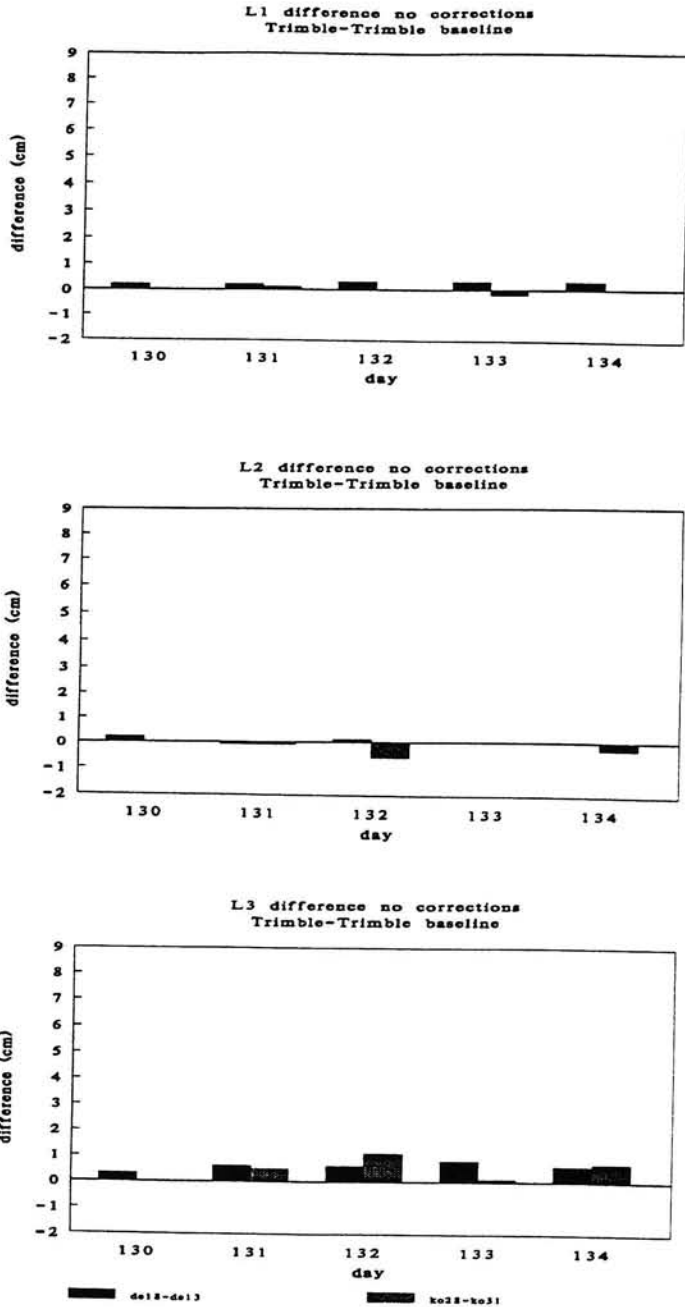


Figure 4.3b: Vertical non-mixed Trimble-Trimble baseline results with no corrections applied.

3.19-3.20). Notice that the Rogue phase center variations are determined for the elevation-range -90/90 degrees. The TurboRogue-Trimble Kootwijk baseline results for day 134 are not taken into account because its solutions are not representative compared with the other days. This is probably caused by the different observation times for the Kootwijk stations between Trimble and TurboRogue for this day. So at the same time no data can be correlated between TurboRogue and Trimble, resulting in the different processed solutions. The baseline results are given in Figure 4.4. The phase center corrections remove much of the effect shown in Figure 4.3a.

Figure 4.5 shows the baseline results with phase center corrections determined for the elevation-range -90/90 degrees. The phase center corrections introduced in the software are for the Trimble and Rogue antenna the Schupler corrections, see Figures 3.17 and 3.18 (Trimble) and Figures 3.19 and 3.20 (Rogue). The phase center corrections for the TurboRogue antenna are the corrections determined at DUCAT for the elevation-range of interest -90/90 degrees (see Figures 3.8 and 3.9). The effect for all mixed baselines is now reduced to about 1 cm difference or less between NoTrop and TropEst for L1, L2 and L3.

Two other combinations with the ESTEC-Rogue phase center corrections are examined. For one combination the ESTEC corrections (Figures 3.21 and 3.22) are introduced for the TurboRogue antenna (elevation-range of interest -75/75 degrees). For the Rogue and Trimble antenna the phase center corrections of Schupler are introduced (elevation-range of interest -90/90 degrees). In this combination we are interested in the results of the T-TR and R-TR baselines. The results of the T-R baseline are the same as the results shown in Figure 4.5. Figure 4.6 shows the differences between NoTrop and TropEst. The L1, L2 and L3 differences are also here reduced to about 1 cm or less. For the other combination the same ESTEC corrections are now introduced for the Rogue antenna (elevation-range of interest -75/75 degrees). For the TurboRogue DUCAT corrections are applied (-90/90 degrees) and for the Trimble Schupler corrections are applied (-90/90 degrees). Figure 4.7 shows the differences between NoTrop and TropEst. The L1, L2 and L3 differences for this combination are larger than the differences shown in Figure 4.6.

### 4.3 Mixed-Baseline results of former studies

The problem with mixing antennas was also investigated by Chris Rocken from UNAVCO [11]. He processed data from a 1.6 meter baseline with and without tropospheric delay parameters. On one end of the baseline a TurboRogue (TR) receiver with a Dorne-Margolin antenna plus choke ring (DM) was placed and at the other end of the baseline a Trimble SSE receiver with Trimble 4000ST antenna (TSST) was placed.

Table 4.2 verifies the cm-error effect. Vertical L1, L2 and L3 solutions agree within 0.8 cm when no tropospheric (No Trop.) parameter is estimated. Vertical L1, L2 and L3 solutions vary about 7 cm when a tropospheric delay parameter is estimated (Trop.Est.).

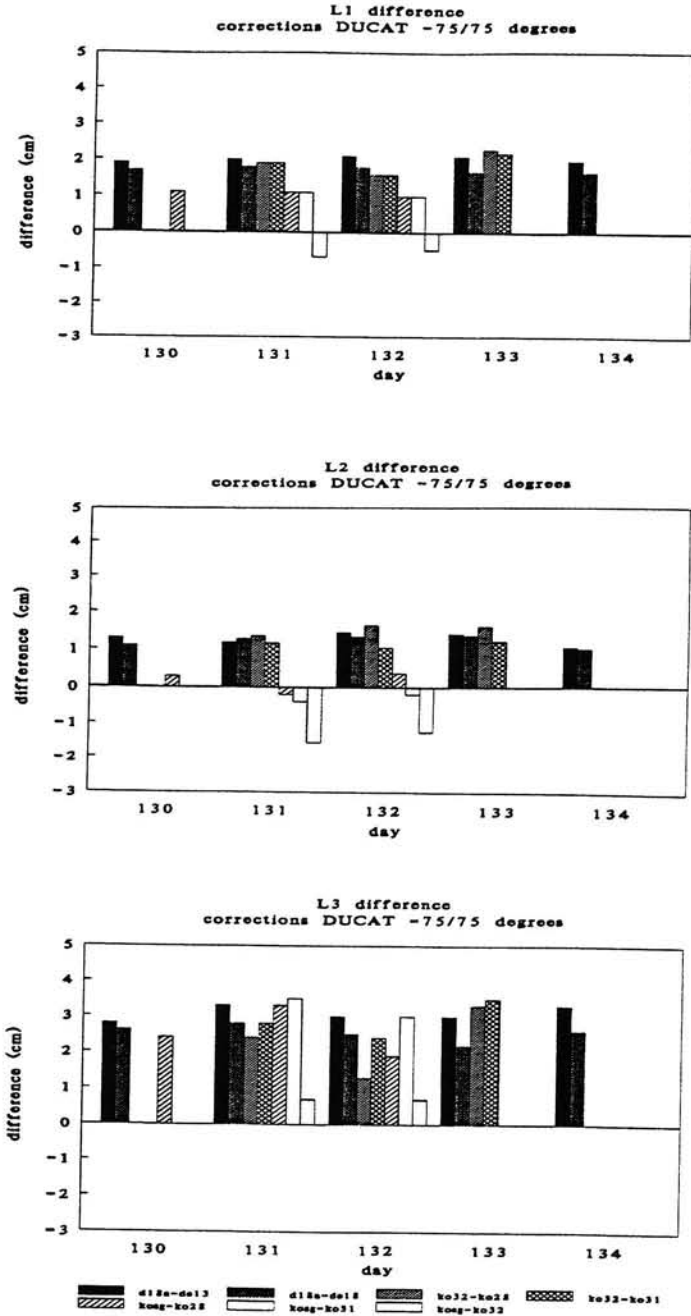


**Figure 4.4:** Vertical mixed-baseline results with DUCAT corrections (-75/75 degrees) for TurboRogue and Trimble, and Schupler corrections (-90/90 degrees) for Rogue applied.

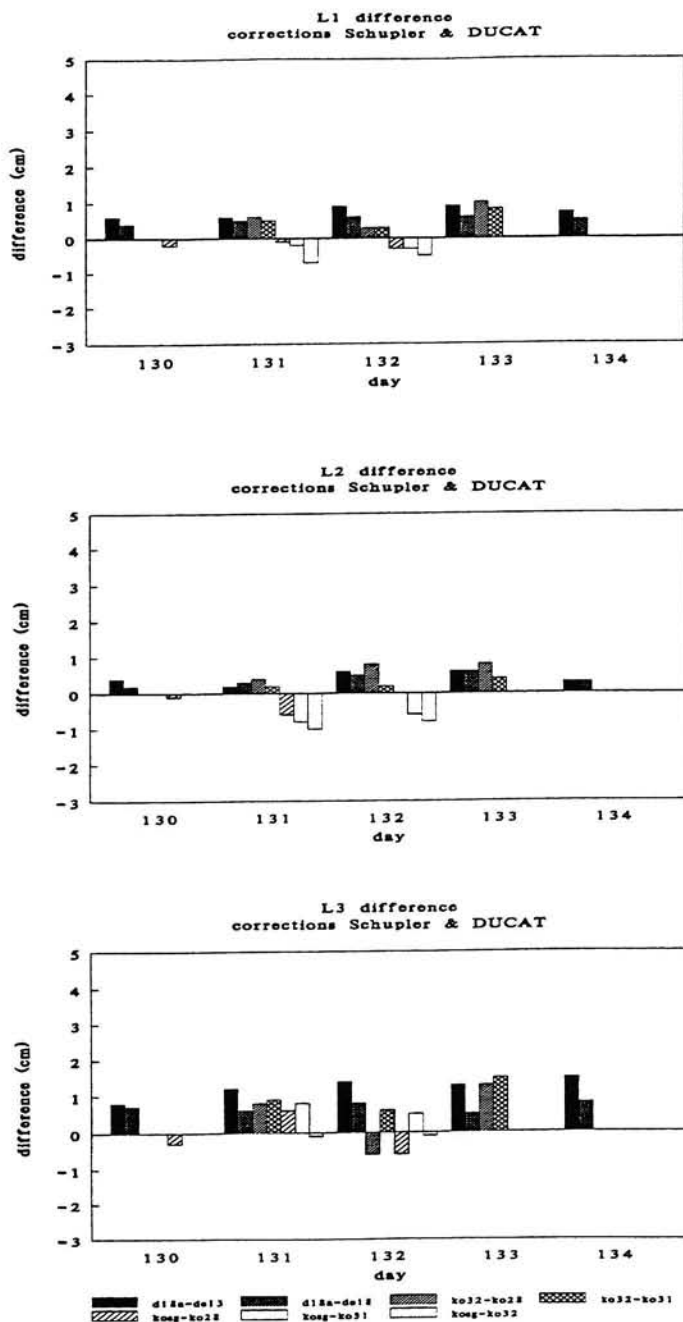
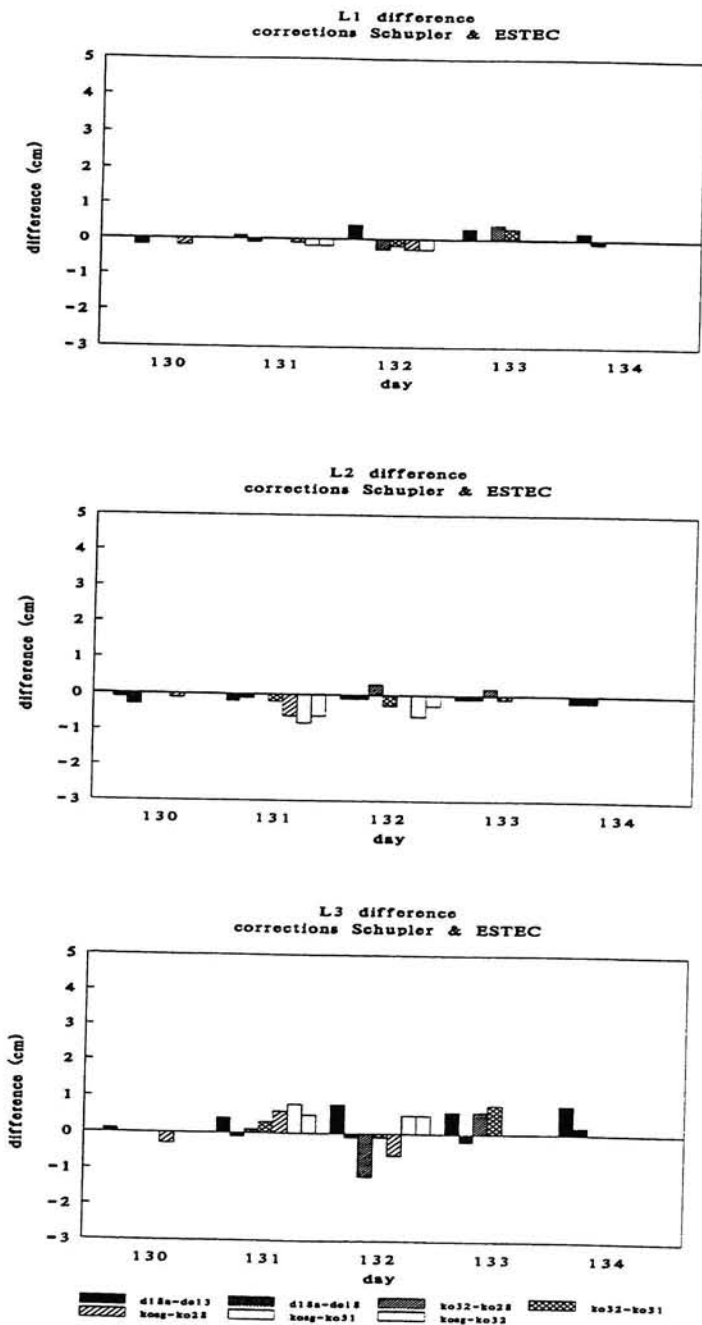
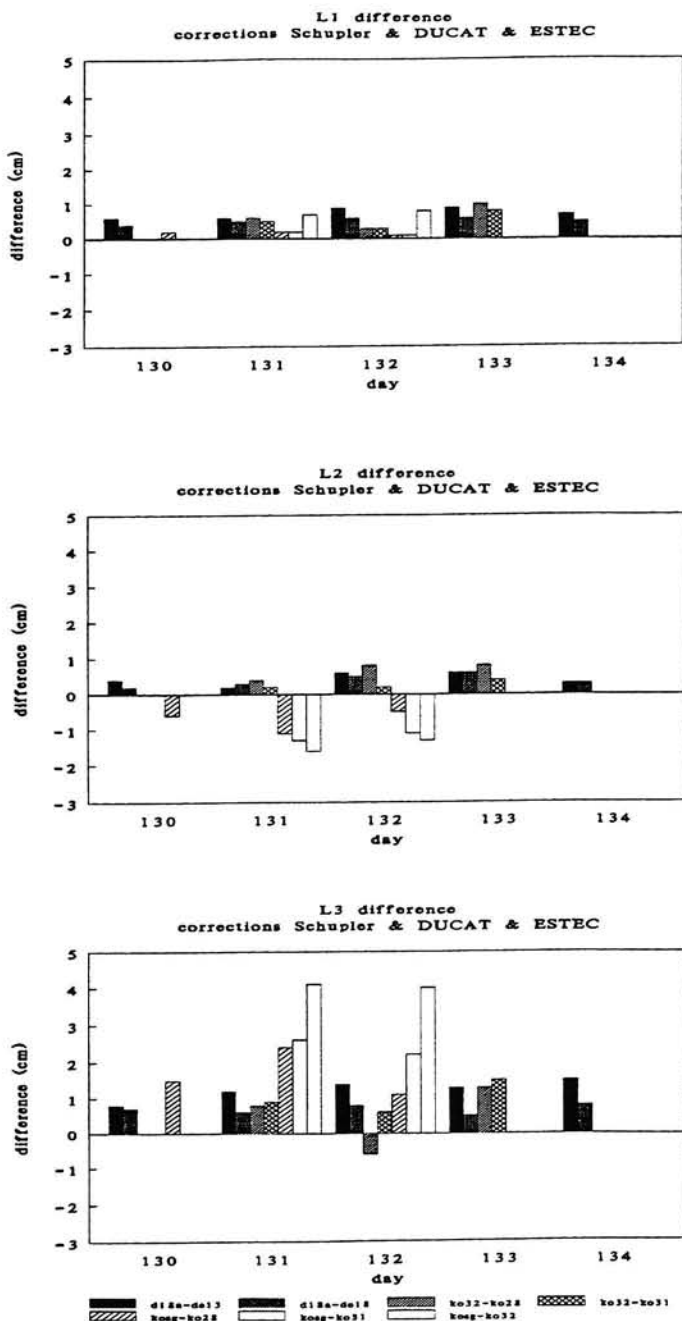


Figure 4.5: Vertical mixed-baseline results with Schupler corrections (-90/90 degrees) for Rogue and Trimble, and DUCAT corrections (-90/90 degrees) for TurboRogue applied.



**Figure 4.6:** Vertical mixed-baseline results with Schupler corrections (-90/90 degrees) for Rogue and Trimble, and ESTEC (Rogue) corrections (-75/75 degrees) for TurboRogue applied.



**Figure 4.7:** Vertical mixed-baseline results with Schupler corrections (-90/90 degrees) for Trimble, DUCAT corrections (-90/90 degrees) for TurboRogue, and ESTEC (Rogue) corrections (-75/75 degrees) for Rogue applied.

The baseline length and horizontal components of the baseline are not strongly affected.

**Table 4.2:** Effect of Trop.Estimation on short TurboRogue-Trimble baseline.

	Height 1600 + [m]			Baseline Length [m]		
	NoTrop	TropEst	difference	NoTrop	TropEst	difference
L1	6.9606	6.9942	0.0336	1.6288	1.6268	0.0020
L2	6.9578	6.9669	0.0091	1.6278	1.6271	0.0007
L3	6.9650	7.0364	0.0714	1.6305	1.6273	0.0032

Chris Rocken used the elevation angle dependent phase center variations determined by Schupler et al. for the phase center corrections. Table 4.3 shows the effect of tropospheric estimation on the same baseline with mixed antennas applying elevation angle dependent corrections.

**Table 4.3:** Effect on TurboRogue-Trimble baseline with phase center corrections.

	Height 1600 + [m]			Baseline Length [m]		
	NoTrop	TropEst	difference	NoTrop	TropEst	difference
L1	6.9594	6.9569	0.0025	1.6276	1.6277	0.0001
L2	6.9516	6.9503	0.0013	1.6277	1.6278	0.0001
L3	6.9716	6.9699	0.0017	1.6275	1.6276	0.0001

The elevation dependent phase center corrections remove much of the effect shown in Table 4.2. The differences in L1, L2 and L3 are, as the results obtained in this study, also affected by an error in the constant phase center offset values (see section 4.4, Table 4.6).

During the IGS campaign at CODE [12] a baseline Wettzell-Zimmerwald (476 km) was used. In Zimmerwald a Trimble SST receiver was installed and in Wettzell a Rogue receiver. From the measurements a constant height difference of 10 cm was found. To test the height problem with the baseline Wettzell-Zimmerwald, an other receiver type, an Ashtech P-code receiver, was installed in Zimmerwald. Table 4.4 shows a summary of the results of the different baselines. The baseline between the Trimble and the Ashtech is accurate at the mm level and the baseline between the Trimble and Wettzell once again shows the 10 cm offset in height but the baseline between the Ashtech and Wettzell shows no offset in height. This means that the results are inconsistent. The only difference in processing these baselines is that for the Ashtech-Trimble baseline (6 m) no tropospheric

parameters are estimated. Therefore this baseline was processed with estimation of tropospheric parameters. Now this baseline shows a difference of 10 cm (see Table 4.4). In Graz an other Ashtech P-code receiver was installed, and the receiver combination Ashtech-Rogue could also be tested. The results with and without estimated tropospheric parameters are given in Table 4.5.

**Table 4.4:** Processing results Wetzell-Zimmerwald.

Baseline	Length [km]	Height difference [mm]
WZZA	476	-11.8
WZZI	476	122.6
ZIZA	0	1.3
ZIZA*	0	-117.5
* Baseline with tropospheric parameters estimated		
WZZA = Wetzell-Zimmerwald Ashtech		
WZZI = Wetzell-Zimmerwald Trimble		
ZIZA = Trimble-Ashtech (both Zimmerwald)		

**Table 4.5:** Processing results Rogue-Ashtech in Graz.

Baseline	Length [km]	Height difference [mm]
GZGA	0	16.6
GZGA*	0	25.0
* Baseline with tropospheric parameters estimated		
GZGA = Wetzell-Zimmerwald Ashtech		

The conclusion to be drawn from the above results is that the Trimble SST antenna must show a strong and different phase center variation with elevation when compared with the phase center variation of the Rogue and Ashtech antenna. This variation being such that it is interpreted by the GPS processing software as tropospheric delay if tropospheric delay parameters are estimated. To test this the Trimble-Ashtech combination in Zimmerwald was again processed. For this test all ambiguities were resolved. Thereafter L1, L2 and L3 frequencies were processed for selected elevations. One started an elevation window between 20 and 40 degrees and shifted this window with 5 degrees until a window of 60 to 80 degrees was reached. The results are plotted in Figure 4.8. The same was done for the Ashtech-Rogue combination in Graz. Those results are plotted in Figure 4.9, notice the large difference in scale between the two figures.

### Trimble-Ashtec

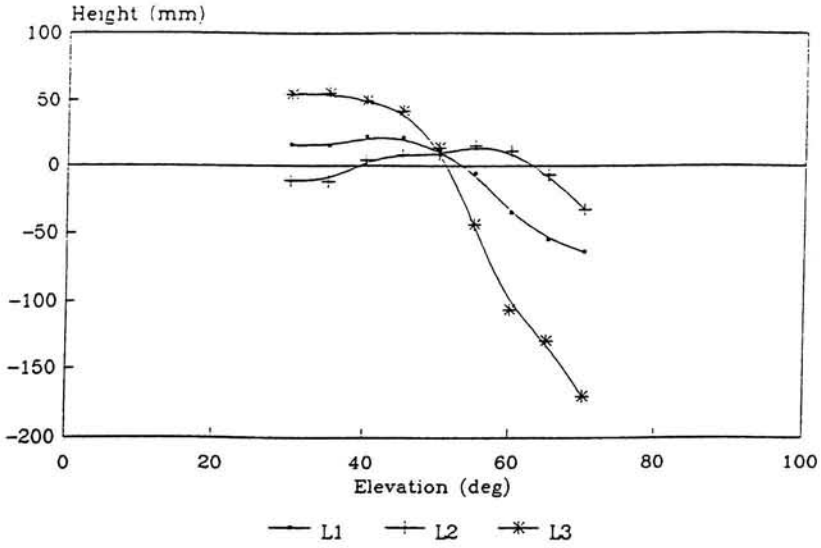


Figure 4.8: Height variation with elevation for Trimble-Ashtec combination.

### Ashtec-Rogue

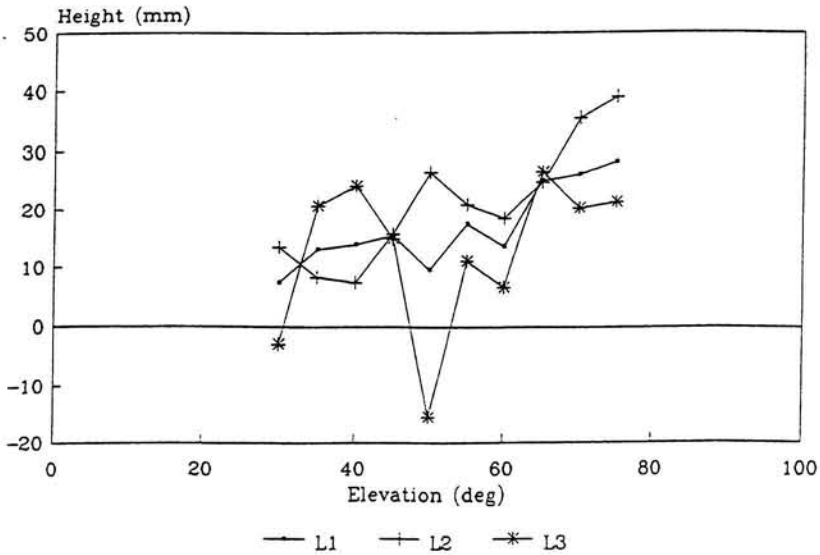


Figure 4.9: Height variation with elevation for Ashtec-Rogue combination.

## 4.4 Discussion

In this section the results of the baselines with different phase center correction combinations given in the previous sections are discussed. In general, all phase center correction combinations show a reduction of the difference between NoTrop and TropEst, but the reductions are not the same for all combinations. Each combination will be discussed and compared with other combinations.

In the baseline results, shown in Figure 4.4, the TR-T and R-T baselines show smaller differences between NoTrop and TropEst when phase center corrections (-75/75 degrees elevation-range) determined at the DUCAT chamber are applied. The R-TR baseline results show roughly the same differences between NoTrop and TropEst, when compared with the R-TR results without phase center corrections. So comparison indicates no significant differences between TurboRogue and Rogue. This phase center correction combination still shows differences for L1, L2 and L3 TR-T and R-T baselines. This can indicate that the Trimble and TurboRogue phase center corrections determined at the DUCAT chamber for an elevation-range of -75/75 degrees do not describe the real pattern of the phase center for L1 and L2. To verify if the L1 and L2 phase center variations of the Trimble and TurboRogue antenna are better described when an elevation-range of interest of -90/90 degrees is considered, the DUCAT Trimble phase center corrections are replaced by the Schupler corrections. Schupler determined the minimum phase center variations for the Trimble considering an elevation-range of interest of -90/90 degrees. The DUCAT TurboRogue phase center corrections are replaced by the DUCAT phase center corrections determined for elevation-range of interest -90/90 degrees. The results are shown in Figure 4.5.

In the baseline results, shown in Figure 4.5, the applied phase center variation combination shows a smaller difference in L1, L2 and L3 for the TR-T and R-T baselines compared to the previous combination. It seems that the Trimble and TurboRogue phase center patterns are better described when a elevation-range of -90/90 degrees is taken into account even-though data with 15 degrees elevation cut-off is used. Furthermore, the R-TR results show that TurboRogue and Rogue have probably the same phase center characteristics, since the solutions are roughly the same when compared with the previous results.

To our surprise we found also good results with the combination Schupler (Trimble and Rogue) and ESTEC (TurboRogue) shown in Figure 4.6. The differences of the TR-T baseline between NoTrop and TropEst are a little bit smaller than the results found with the previous combination (Figure 4.5). But between the Figures 4.5 and 4.6 no significant difference can be seen to conclude which combination is the best. In both cases the differences are at centimeter level or less. Comparison of the Figures 4.5 and 4.6 with the previous combinations show that the differences between Figures 4.5 and 4.6 are roughly the same. The results of the R-TR baseline difference between NoTrop and TropEst are for L1, L2 and L3 not much affected when compared with the previous combination. Since Rogue corrections are applied for a TurboRogue antenna, the differences between

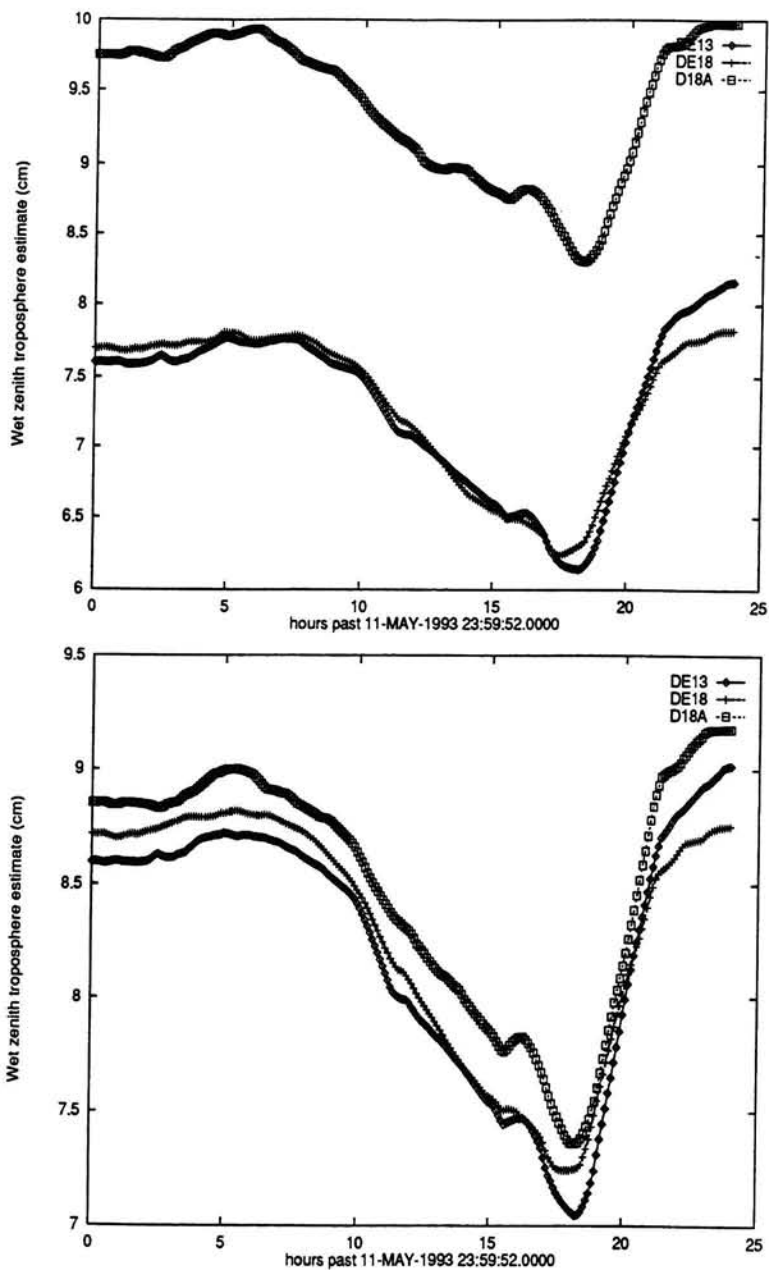


**Figure 4.10:** Estimated wet troposphere parameter for day 132 without (a), and (b) with phase center corrections for Delft.

the Rogue and TurboRogue phase patterns, shown in chapter 3, are apparently not significantly different enough to speak about two different antennas. Remarkable for this combination is that the ESTEC-Rogue phase pattern shows a minimum variation for elevation-range of interest  $-75/75$  degrees. While in the previous combinations we have shown that the differences between NoTrop and TropEst are smaller when an elevation-range of  $-90/90$  degrees for all antennas is considered. Fig 4.7 verifies this. In this combination the baselines including Rogue antenna show larger differences between NoTrop and TropEst. Here we apply for the Rogue antenna phase center corrections which show a minimum phase variation for elevation-range of interest  $-75/75$  degrees. While for Trimble and TurboRogue phase center corrections determined for elevation-range  $-90/90$  degrees are applied.

In Figures 4.10 and 4.11 we can see the interpretation of the phase center as a tropospheric delay when different antennas are involved. The figures show the estimated wet troposphere parameter for day 132 with and without phase center corrections for Delft and Kootwijk respectively. The figures show different estimates for stations with different antennas when no corrections are applied. Between Trimble antennas the values roughly correspond with each other. Notice that station KO32 has for day 132 a small number of observations. The estimates for the different stations are roughly the same when the phase center corrections are applied.

The L1, L2 and L3 NoTrop and TropEst solutions show a constant offset of the height-component for the mixed baselines. For the TR-T baseline of the phase center correction combination shown in Figure 4.6, this offset is for L1, L2 and L3 of about 1.7, 1.5 and 1.9 cm respectively, see Table 4.6. The results show differences between L1, L2 and L3 solutions if tropospheric parameters are estimated or not. These differences are caused by the normalization of the phase center variation. The normalized pattern shows a phase center variation in which the measured phase difference at zenith is set at zero. It is possible that there exists an offset of the phase center at zenith between L1 and L2 phase center, so the real pattern of the phase center is a translation of the pattern (see Figure 4.12). This means that the introduced constant phase center offset values must be changed according to the translation.

**Table 4.6:** TurboRogue-Trimble baseline results of the height component with ESTEC and Schupler phase center corrections (see Figure 4.6) for day 131.

ko32-ko28	NoTrop (m)	TropEst (m)	difference
L1	.0167	.0166	-.0001
L2	.0149	.0144	-.0005
L3	.0192	.0198	.0006
ko32-ko31	NoTrop (m)	TropEst (m)	difference
L1	.0176	.0173	-.0003
L2	.0165	.0142	-.0023
L3	.0192	.0221	.0029

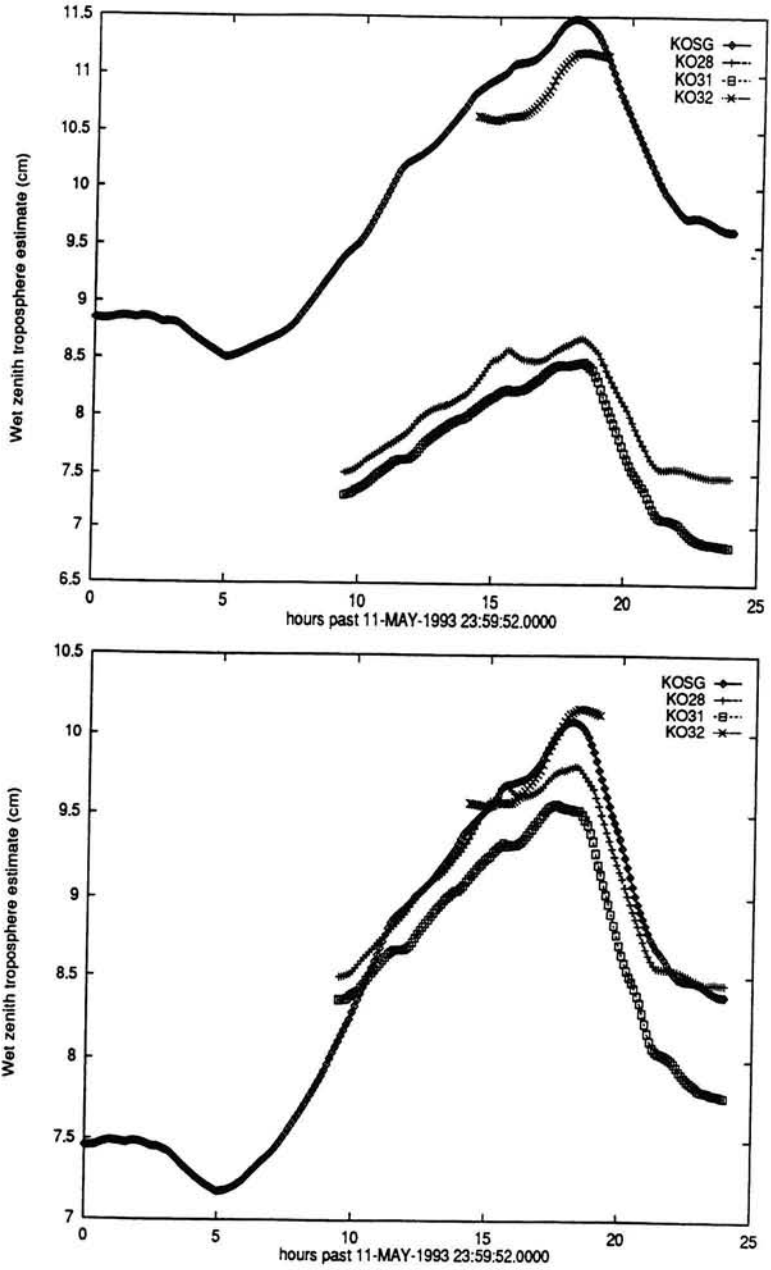


**Figure 4.11:** Estimated wet troposphere parameter for day 132 (a) without, and (b) with phase center corrections for Kootwijk.

The results of Chris Rocken (UNAVCO) show that the difference is removed when Rogue phase center corrections determined by Schupler are introduced for the TurboRogue antenna. In our case we find the best results when phase center corrections determined at ESTEC (Rogue) or at DUCAT (TurboRogue) are applied to the TurboRogue. Although small differences between Rogue and TurboRogue seem to exist, the processed results do not show a clear difference between these two antennas. Since Chris Rocken applied Rogue measurements for a TurboRogue antenna, the phase patterns of the Rogue and TurboRogue antenna can be considered as the same. The results of Chris Rocken and the results of this study show that the difference is removed when Trimble phase center corrections determined by Schupler are used.

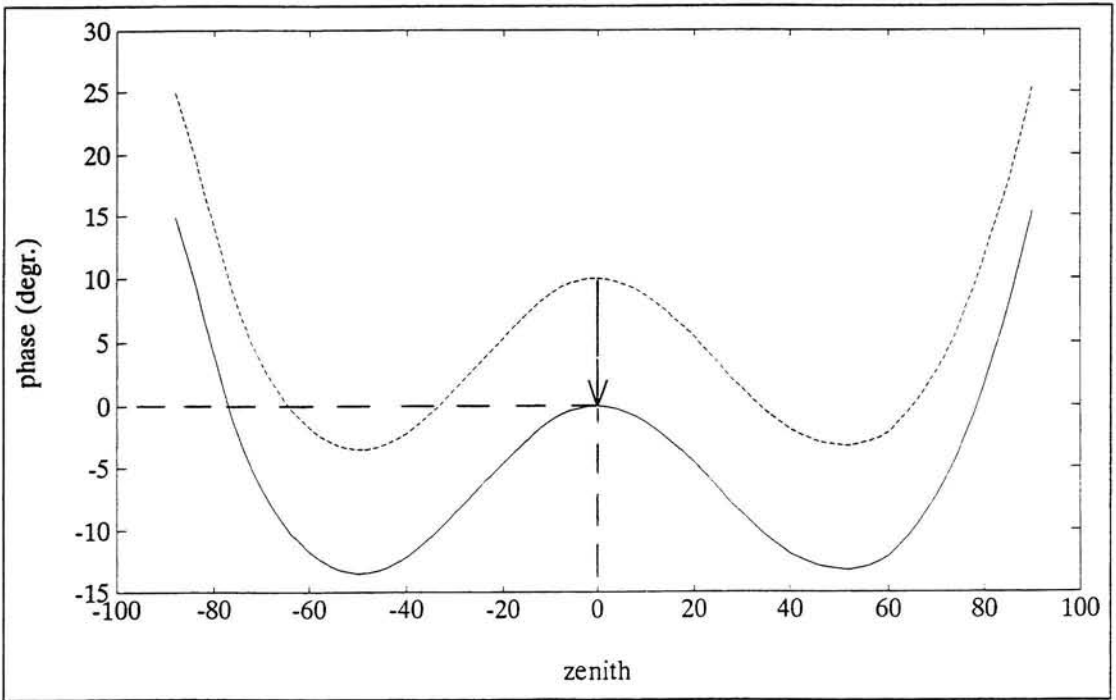


Figure 4.12: Normalization of the phase pattern.



# 5. Conclusions and Recommendations

## 5.1 Conclusions

From the results of the measurements performed at DUCAT can be concluded that the Trimble and TurboRogue antenna are two different antennas. Both show different phase center variations and different averaged phase center offsets.

The minimum phase center variation can be determined when the elevation-range of interest is taken into account. Different phase center variations and averaged phase center offsets for the same antenna are found for different range-elevations of interest, so the determination of the minimum phase center variation is ambiguous. Comparison between phase center variations of same antenna types and different antenna types can only be done if the same elevation-range of interest is taken into account for all involved antennas.

From the results of the processed data can be concluded that mixing of Trimble with TurboRogue and Rogue leads to a height error of approximately 8 cm when tropospheric parameters are estimated. This tropospheric error is reduced to sub-centimeter level when direction dependent phase center corrections are applied. Mixing of TurboRogue with Rogue leads to a height error of approximately 2 cm when tropospheric parameters are estimated. A clear reduction of this error is not obtained when phase center corrections are applied.

Differences between Rogue and TurboRogue phase center patterns may exist. Both antennas show small differences of the phase center variation when for both antennas the same elevation-range of interest is considered. But from the processed baseline results we have seen that these differences are not significantly enough to exclude the possibility that TurboRogue and Rogue are not identical. Concerning the Trimble antenna, mixed-baselines with the smallest differences when troposphere parameters are estimated or not, are obtained when phase center corrections determined by Schupler are applied. The Trimble antenna shows larger azimuthal phase center variations than the TurboRogue and Rogue antenna. Non-mixed Trimble-Trimble results show that between antennas of the same type the phase center variations are the same.

The best results are obtained for two combinations of phase center corrections. One combination is: the phase center corrections determined by Schupler for the Trimble, the phase center corrections determined by Schupler for the Rogue, and the phase center corrections determined in this study at the DUCAT chamber for the TurboRogue. For this combination an elevation-range of interest of -90/90 degrees is valid for all three antennas. The second combination is the same as the first one, except that for the TurboRogue the phase center corrections determined by ESTEC are used. The last combination is typical, because the ESTEC-Rogue phase center corrections show minimum phase center variations

valid for the elevation-range of interest  $-75/75$  degrees. Therefore, it is difficult to determine which minimum phase center variation must be used for corrections of the TurboRogue phase center. But Chris Rocken used Schupler-Rogue phase center corrections for a TurboRogue antenna resulting in a large reduction of the tropospheric error. The Schupler phase variation is valid for elevation-range  $-90/90$  degrees. So comparison of all examined combinations in this study shows that the antenna phase center variation is better described when an  $-90/90$  degrees elevation-range of interest is considered.

An error in the offset in the L1, L2 and L3 solutions of the estimated baselines appears. The error is caused by the normalization of the phase center variation patterns. Normalization of the phase pattern produces a constant shift of the measured phase at each elevation angle. The measured phase at zenith is set at zero. This places the apparent phase center at zenith on the determined averaged phase center. In other words, the normalized phase pattern shows the relative variation of the phase center, with the averaged phase center as reference point.

## 5.2 Recommendations

The minimum phase center variation of the different antennas can not be determined if the elevation-range of interest is not taken into account. Different minimum phase center variations are found for different elevation-range of interest. It is impossible to say which phase center variation is the right one, because all possible variations are correct. The problem is caused by the technique used for the determination of the averaged phase center and its variation. This technique says that the phase center is determined when a minimum phase shift of the phase center pattern is found. As shown in chapter 3, different minimum phase patterns are found for different elevation-ranges of interest for the same antenna. A possible different technique to avoid this problem is the following (see Figure 5.1): Divide the total elevation-range from  $-90$  to  $90$  degrees into small regions (for example:  $0-5$  degrees). For each region the averaged phase center of the antenna is determined by measuring its minimum phase center variation in that specific region. The measurement is repeated for each region. The result is a different determined average phase center for each region. The variation of all averaged phase centers can be determined with respect to a reference phase center, this can be the averaged phase center at zenith, see Figure 5.2. This is the elevation dependent phase center variation which can be used for the phase center corrections when troposphere parameters are estimated. This technique is not found in literature and should be tested.

A better understanding of the phase center characteristics of different antenna types and antennas of the same type can be achieved when more antennas are involved for phase center test-measurements. It is possible that the phase center variations of the antennas located at the stations can have different phase center characteristics than the tested antennas at DUCAT, ESTEC and Schupler. So the phase center corrections applied in this study to the antennas of the stations do not have to represent the real values. The processed baseline solutions would be more reliable when all antennas of the stations were tested in an anechoic chamber.

In this study we have determined the antenna phase center in an anechoic chamber. The possibility exist to calibrate the antennas based on GPS data. The interpreted 'tropospheric delay' can be translated into a change of the phase center position.

A network consisting of a larger number of stations than Kootwijk or Delft can produce more possible non-mixed and mixed baselines. Such network can provide more information about the solutions of the baselines. Also the number of days during a measurement campaign can be augmented. More days can give more information.

Finally, in this study the determination of the antenna phase center is achieved without analytical formulations. Analytical formulations are usually very laborious and exist only for a limited number of configurations. To get a better understanding about the antenna phase center, a theoretical model of the phase center should be developed in the future. This model can be compared with the antenna measurements.

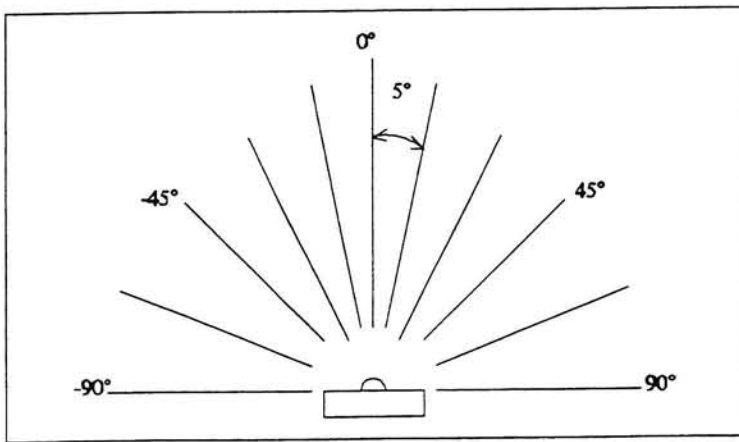


Figure 5.1: Different technique avoiding the elevation-range of interest.

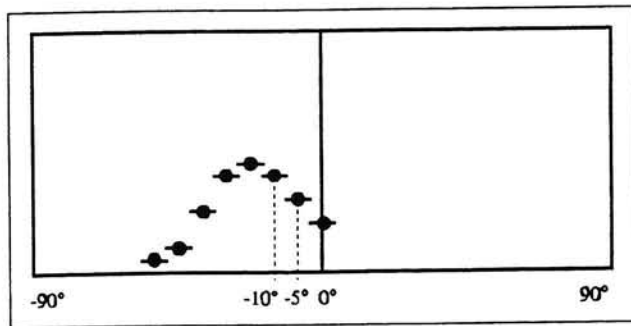


Figure 5.2: Variation of the averaged phase centers.



## 6. References

- [1] Brouwer, F.J.J.; Navigatie en geodetische puntsbepaling met het Global positioning System; TU Delft, Faculteit der Geodesie; 1992; Delft, The Netherlands
- [2] Hofmann-Wellenhof, B.; Global Positioning System, Theory and practice; Springer; 1992; Wien, Austria
- [3] Wells, D.; Guide to GPS positioning; Canadian GPS associates; 1986; Fredericton, Canada
- [4] Seeber, G.; Satellite geodesy; De Gruyter; 1993; Berlin, Germany
- [5] Jong, C.D. de; GPS-satellite orbits and atmospheric effects; TU Delft, Faculteit der Geodesie; 1991; Delft, The Netherlands
- [6] Balanis, C.A.; Antenna Theory; Harper and Row; 1982; New York, U.S.A.
- [7] Weeks, W.L.; Antenna engineering; McGraw-Hill inc.; 1968; U.S.A.
- [8] Blake, L.V.; Antennas; John Wiley & Sons inc.; 1966; New York, U.S.A.
- [9] L.P. Ligthart, G.J.H. Luyten and P.J.F. Swart; Antenna and radar cross section measurement facility at the Delft University of Technology; Delft, The Netherlands
- [10] Rocken, C.; GPS Antenna Mixing Problems; UNAVCO GPS community; November 12, 1992
- [11] Schupler et al.; A Consumer's Report on GPS Antennas; CDP Investigators Meeting, October 25, 1990
- [12] Springer T. and Gurtner W.; Trimble antenna phase center problem, Astronomical Institut, University of Berne, Switzerland
- [13] ESTEC; Rogue Antenna Measurements; November, 1990; Noordwijk, The Netherlands



## Series 01: Aerodynamics

01. F. Motallebi, 'Prediction of Mean Flow Data for Adiabatic 2-D Compressible Turbulent Boundary Layers'  
1997 / VI + 90 pages / ISBN 90-407-1564-5
02. P.E. Skåre, 'Flow Measurements for an Afterbody in a Vertical Wind Tunnel'  
1997 / XIV + 98 pages / ISBN 90-407-1565-3
03. B.W. van Oudheusden, 'Investigation of Large-Amplitude 1-DOF Rotational Galloping'  
1998 / IV + 100 pages / ISBN 90-407-1566-1
04. E.M. Houtman / W.J. Bannink / B.H. Timmerman, 'Experimental and Computational Study of a Blunt Cylinder-Flare Model in High Supersonic Flow'  
1998 / VIII + 40 pages / ISBN 90-407-1567-X
05. G.J.D. Zondervan, 'A Review of Propeller Modelling Techniques Based on Euler Methods'  
1998 / IV + 84 pages / ISBN 90-407-1568-8
06. M.J. Tummers / D.M. Passchier, 'Spectral Analysis of Individual Realization LDA Data'  
1998 / VIII + 36 pages / ISBN 90-407-1569-6
07. P.J.J. Moeleker, 'Linear Temporal Stability Analysis'  
1998 / VI + 74 pages / ISBN 90-407-1570-X
08. B.W. van Oudheusden, 'Galloping Behaviour of an Aeroelastic Oscillator with Two Degrees of Freedom'  
1998 / IV + 128 pages / ISBN 90-407-1571-8
09. R. Mayer, 'Orientation on Quantitative IR-thermography in Wall-shear Stress Measurements'  
1998 / XII + 108 pages / ISBN 90-407-1572-6
10. K.J.A. Westin / R.A.W.M. Henkes, 'Prediction of Bypass Transition with Differential Reynolds Stress Models'  
1998 / VI + 78 pages / ISBN 90-407-1573-4
11. J.L.M. Nijholt, 'Design of a Michelson Interferometer for Quantitative Refraction Index Profile Measurements'  
1998 / 30 pages / ISBN 90-407-1574-2
12. R.A.W.M. Henkes / J.L. van Ingen, 'Overview of Stability and Transition in External Aerodynamics'  
1998 / IV + 48 pages / ISBN 90-407-1575-0
13. R.A.W.M. Henkes, 'Overview of Turbulence Models for External Aerodynamics'  
1998 / IV + 40 pages / ISBN 90-407-1576-9

## **Series 02: Flight Mechanics**

01. E. Obert, 'A Method for the Determination of the Effect of Propeller Slipstream on a Static Longitudinal Stability and Control of Multi-engined Aircraft'  
1997 / IV + 276 pages / ISBN 90-407-1577-7
02. C. Bill / F. van Dalen / A. Rothwell, 'Aircraft Design and Analysis System (ADAS)'  
1997 / X + 222 pages / ISBN 90-407-1578-5
03. E. Torenbeek, 'Optimum Cruise Performance of Subsonic Transport Aircraft'  
1998 / X + 66 pages / ISBN 90-407-1579-3

## **Series 03: Control and Simulation**

01. J.C. Gibson, 'The Definition, Understanding and Design of Aircraft Handling Qualities'  
1997 / X + 162 pages / ISBN 90-407-1580-7
02. E.A. Lomonova, 'A System Look at Electromechanical Actuation for Primary Flight Control'  
1997 / XIV + 110 pages / ISBN 90-407-1581-5
03. C.A.A.M. van der Linden, 'DASMAT-Delft University Aircraft Simulation Model and Analysis Tool. A Matlab/Simulink Environment for Flight Dynamics and Control Analysis'  
1998 / XII + 220 pages / ISBN 90-407-1582-3

## **Series 05: Aerospace Structures and Computational Mechanics**

01. A.J. van Eekelen, 'Review and Selection of Methods for Structural Reliability Analysis'  
1997 / XIV + 50 pages / ISBN 90-407-1583-1
02. M.E. Heerschap, 'User's Manual for the Computer Program Cufus. Quick Design Procedure for a CUt-out in a FUSelage version 1.0'  
1997 / VIII + 144 pages / ISBN 90-407-1584-X
03. C. Wohlever, 'A Preliminary Evaluation of the B2000 Nonlinear Shell Element Q8N.SM'  
1998 / IV + 44 pages / ISBN 90-407-1585-8
04. L. Gunawan, 'Imperfections Measurements of a Perfect Shell with Specially Designed Equipment (UNIVIMP)  
1998 / VIII + 52 pages / ISBN 90-407-1586-6

## Series 07: Aerospace Materials

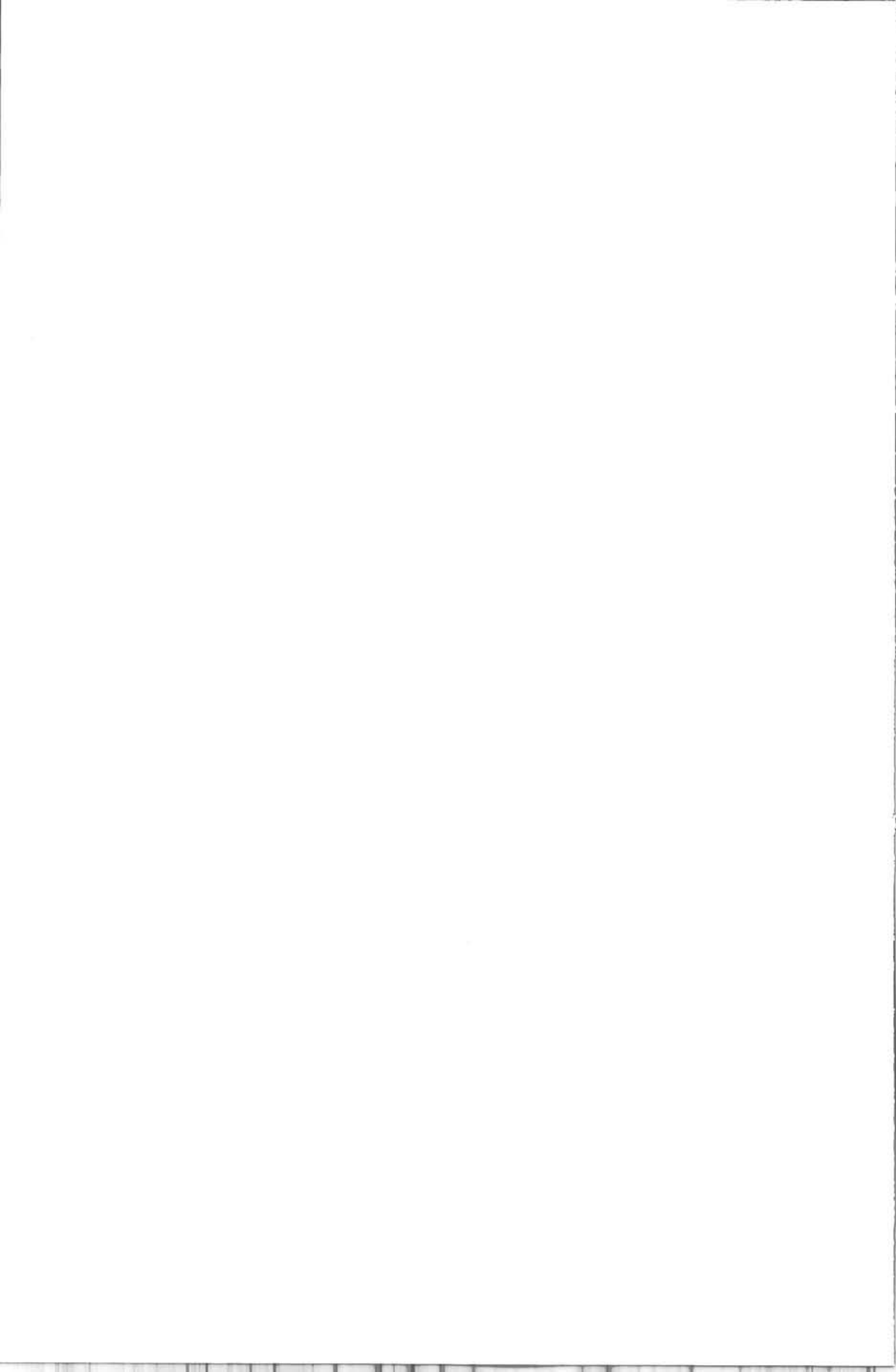
01. A. Vašek / J. Schijve, 'Residual Strength of Cracked 7075 T6 Al-alloy Sheets under High Loading Rates'  
1997 / VI + 70 pages / ISBN 90-407-1587-4
02. I. Kunes, 'FEM Modelling of Elastoplastic Stress and Strain Field in Centre-cracked Plate'  
1997 / IV + 32 pages / ISBN 90-407-1588-2
03. K. Verolme, 'The Initial Buckling Behavior of Flat and Curved Fiber Metal Laminate Panels'  
1998 / VIII + 60 pages / ISBN 90-407-1589-0
04. P.W.C. Provó Kluit, 'A New Method of Impregnating PEI Sheets for the *In-Situ* Foaming of Sandwiches'  
1998 / IV + 28 pages / ISBN 90-407-1590-4
05. A. Vlot / T. Soerjanto / I. Yeri / J.A. Schelling, 'Residual Thermal Stresses around Bonded Fibre Metal Laminate Repair Patches on an Aircraft Fuselage'  
1998 / IV + 24 pages / ISBN 90-407-1591-2
06. A. Vlot, 'High Strain Rate Tests on Fibre Metal Laminates'  
1998 / IV + 44 pages / ISBN 90-407-1592-0
07. S. Fawaz, 'Application of the Virtual Crack Closure Technique to Calculate Stress Intensity Factors for Through Cracks with an Oblique Elliptical Crack Front'  
1998 / VIII + 56 pages / ISBN 90-407-1593-9
08. J. Schijve, 'Fatigue Specimens for Sheet and Plate Material'  
1998 / VI + 18 pages / ISBN 90-407-1594-7

## Series 08: Astrodynamics and Satellite Systems

01. E. Mooij, 'The Motion of a Vehicle in a Planetary Atmosphere'  
1997 / XVI + 156 pages / ISBN 90-407-1595-5
02. G.A. Bartels, 'GPS-Antenna Phase Center Measurements Performed in an Anechoic Chamber'  
1997 / X + 70 pages / ISBN 90-407-1596-3
03. E. Mooij, 'Linear Quadratic Regulator Design for an Unpowered, Winged Re-entry Vehicle'  
1998 / X + 154 pages / ISBN 90-407-1597-1







3021892

This report gives the measurements results of the evaluation and azimuth angle dependent phase center variations of a Turbo Rogue and a Trimble GPS antenna, performed in an anechoic chamber. The measurements were made for the L 1 and L 2 carrier phase frequencies. Results of the measurements show different phase center variations are found for the same antenna when the elevation-range of interest is taken into account. Short baseline measurements are processed including the measured phase center variations for the different antennas. It will be shown that calibration of the phase center variations using the results from phase center measurement in an anechoic chamber removes the major part of the vertical baseline error when different antennas are involved.

ISBN 90-407-1596-3



9 799040 715968

